NATIONAL ADVISORY COMMITTEE FOR AERONAUTICS

TECHNICAL NOTE 3048

EXPERIMENTAL INVESTIGATION OF THE EFFECTS OF COOLING ON FRICTION AND ON BOUNDARY-LAYER TRANSITION FOR LOW-SPEED GAS FLOW AT THE ENTRY OF A TUBE

By Stephen J. Kline and Ascher H. Shapiro

Massachusetts Institute of Technology

Washington
November 1953

NATIONAL ADVISORY COMMITTEE FOR AERONAUTICS

TECHNICAL NOTE 3048

EXPERIMENTAL INVESTIGATION OF THE EFFECTS OF COOLING ON FRICTION AND ON BOUNDARY-LAYER TRANSITION FOR LOW-SPEED GAS FLOW AT THE ENTRY OF A TUBE

By Stephen J. Kline and Ascher H. Shapiro

SUMMARY

The effect of cooling on boundary-layer transition in the steady flow of air in the entrance of a smooth round tube has been investigated experimentally. Runs were made at diameter Reynolds numbers varying from 50,000 to 106,000. The levels of disturbance were such as to yield adiabatic length Reynolds numbers (based on the length to the start of transition) ranging from 500,000 to 1,800,000. Transition was determined from logarithmic plots of local apparent friction factor against length Reynolds number. Temperature differences between the wall and the free stream up to 270° F were applied, but no significant effect of cooling on the point of transition was found.

For a gas the theory of stability based on vanishingly small disturbances predicts a large increase in the minimum value of Reynolds number at which the laminar velocity profile first becomes unstable on a flat plate when the plate is cooled. In addition, the theory predicts that the initial rate of amplification of the disturbance is reduced by cooling. Because of pressure gradients, the flow in the entrance of a tube is not exactly the same as that on a flat plate, but the behavior of the flow is thought to be very similar to that on a flat plate when the boundary-layer thickness is small compared with the tube radius, as it was throughout these tests. It appears, therefore, that, in the tests reported here, transition may not have been brought about by amplification of the so-called Tollmien-Schlichting waves of the current laminar instability theory. This suggests that study of the nonlinear terms of the differential equations of motion will be necessary before the mechanism of transition can be fully understood.

The present results indicate that the effect of cooling on transition is not likely to be significant in any normal internal flow. The measured effect on transition, even when only very slight disturbances are present, is always at least one order of magnitude less than the effect theoretically predicted for the point at which the laminar velocity profile first becomes unstable.

All the laminar adiabatic data of these tests are correlated within ±6 percent by the equation

$$4f_{APP}\,Re_D = 6.87\Big/\sqrt{\frac{x/D}{Re_D}}$$

in the range for which $(x/D)/Re_D = Re_x/Re_D^2 \leq 0.005$, where f_{APP} denotes the apparent friction factor; Re_x, the length Reynolds number; Re_D, the diameter Reynolds number; x, the axial distance from the tube entrance; and D, the diameter of the tube. A simple theory based on the momentum integral method and the assumptions of very thin boundary layers having flat-plate-like behavior yields the comparable formula

$$4f_{APP}\,Re_D = 7.15\Big/\sqrt{\frac{x/D}{Re_D}}$$

INTRODUCTION

The theoretical studies of Tollmien (refs. 1 and 2), Schlichting (ref. 3), Prandtl (ref. 4), and others have shown that beyond a certain critical Reynolds number the laminar boundary layer becomes unstable to small disturbances in a certain critical frequency range. This remarkable mathematical theory has been verified beyond question by the experimental work of Schubauer and Skramstad (ref. 5) and of Liepmann (refs. 6 and 7). More recently Lin (ref. 8) and Lees and Lin (ref. 9) have improved the mathematical theory and have extended it to cover the case of the compressible fluid. Lees (ref. 10) and Van Driest (ref. 11) have carried out numerical calculations showing the effect of heating or cooling on the critical Reynolds number at which the boundary layer becomes unstable to small disturbances for the flow of a gas past a flat plate. Both Lees and Van Driest predict the critical Reynolds number in gases to be greatly increased by cooling and greatly decreased by heating. But Van Driest's calculations show much less effect, particularly of cooling, than do those of Lees. The method employed by all these theoretical investigators is to introduce a small perturbation into the differential equations of motion, discard terms involving disturbances to the square, and then determine whether the disturbance increases or dies out with increasing time. The current theory is thus concerned with the point at which the laminar flow becomes unstable to vanishingly small disturbances, but it is unable to predict either the location of the transition point or how a laminar boundary layer behaves in the presence of large disturbances.

In any discussion of transition the distinction between the transition point and the point at which the laminar flow becomes unstable to small disturbances must be kept clearly in mind. At the point where the laminar flow becomes unstable the disturbances present may be very small. In this case turbulence will not appear immediately but will start considerably further downstream after the disturbances have had time to amplify. In this discussion the point at which turbulence first begins to appear and the velocity profile begins to change from laminar to turbulent will be referred to as the transition point. The point at which the laminar profile first becomes unstable will be called the instability point. It should be noted that, if transition occurs by amplification of unstable waves, the transition point must lie at or downstream of the instability point.

In most technical applications the transition point is of interest rather than the instability point. The theory cited above gives no direct information about the transition point. It does predict, however, that the initial amplification of unstable waves is inversely proportional to the one-fourth power of the Reynolds number at the instability point. Thus, if the Reynolds number at the instability point is increased by cooling, one might surmise from the theory that the transition Reynolds number would be increased by an even greater amount. Such a delay of the transition Reynolds number would be of considerable importance in many technical applications, since the heat-transfer and friction coefficients depend strongly on whether the flow is laminar or turbulent. Examples where direct application could be made include (1) cooled turbine blades or airfoil sections, (2) aircraft oil coolers, (3) gas-turbine plant regenerators and intercoolers, and (4) the wings of long-range aircraft.

Since the current theory of instability is unable to predict directly anything regarding the transition point, it is necessary to resort to experiment. The primary purpose of the present study was to investigate the practical possibilities of delaying transition, and thus increasing the transition Reynolds number, by cooling the laminar boundary layer in a gas.

The present investigation was carried out in the entrance zone of a smooth round tube. A tube was used primarily for simplicity. However, many of the important technical applications are actually of this geometry; and, in addition, the flow near the entrance of a tube behaves much like that on a flat plate. The principal difference between the two flows is that a favorable pressure gradient exists in the tube. A secondary objective of the present investigation was to measure and correlate the local apparent friction factor in the entrance zone of a tube.

This work was conducted at the Massachusetts Institute of Technology under the sponsorship and with the financial assistance of the National Advisory Committee for Aeronautics.

SYMBOLS

A cross-sectional area of tube

C_D flow coefficient of contraction nozzle

C_f skin-friction coefficient, $\tau_w \Big/ \frac{1}{2}\rho V^2$

D diameter of tube

$4f_{APP}$ local apparent friction factor, defined by the equation

$$-4f_{APP} \equiv \frac{dp/d(x/D)}{\frac{1}{2}\rho V^2}$$

$4\bar{f}_{APP}$ mean apparent friction factor up to a section $x = L$, defined by the equation

$$4\bar{f}_{APP}\left(\frac{L}{D}\right) \equiv \int_0^{L/D} 4f_{APP}\, d\left(\frac{x}{D}\right) = \frac{p_i - p}{\frac{1}{2}\rho V^2}$$

g conversion constant in Newton's second law

L axial length from entrance of tube for which mean apparent friction factor $4\bar{f}_{APP}$ is evaluated

p static pressure at section x

p_i static pressure at entrance to tube, that is, at $x = 0$

p_o stagnation pressure in stilling chamber

Q volume flow rate through test section

Re_D diameter Reynolds number, based on tube diameter and on free-stream properties, $\rho_o V D / \mu_o$

Re_{x_1} length Reynolds number, based on length from tube entrance and on free-stream properties, $\rho_o V \bar{x} / \mu_o$

Re_{x_2} length Reynolds number, based on length from tube entrance and on fluid properties taken at arithmetic mean of stream and wall temperatures, $\rho_m V \bar{x} / \mu_m$

T_o stagnation temperature in stilling chamber

T_w wall temperature

u axial velocity at any location x and y

u_c axial velocity in frictionless core

V mean one-dimensional velocity in x direction, Q/A

x axial distance from tube entrance

$\bar{x}$ proper mean distance x for a measured value of local apparent friction factor

y radial coordinate in test section measured from wall

δ boundary-layer thickness

μ coefficient of viscosity

ρ mass density

σ dimensionless parameter, $(x/D)/Re_D = Re_x/Re_D^2$

ϕ functional relation

τ_w shear stress at wall

Subscripts:

o free-stream condition (essentially the same as stagnation in these tests)

m mean taken at arithmetic average of wall and stream temperatures

Special terms:

The term "Reynolds number" always means Re_{x_1} unless otherwise stated; Re_D is referred to as "diameter Reynolds number."

The term "transition point" means the point at which the velocity profile begins to deviate significantly from that of laminar flow as evidenced by a change in the local apparent friction factor.

The term "instability point" means the point at which the laminar profile first becomes unstable to a vanishingly small disturbance of any frequency.

DESCRIPTION OF TEST APPARATUS

A flow diagram of the test apparatus is shown in figure 1(a). The main components are the air supply system, air heaters, stilling chamber, test section, and instrumentation. Atmospheric air was used in all tests and was supplied to the test apparatus from a 125-pound-per-square-inch-absolute, 400-cubic-foot-per-minute reciprocating compressor discharging through an aftercooler, receiver tank, and approximately 150 feet of 2-inch pipe. After passing through two 12-kilowatt air heaters in series and through a series of three short-radius elbows, the air was brought into the stilling chamber (fig. 1(b)) by means of a 7° conical diffuser made of sheet metal.

Large-scale disturbances were removed by a honeycomb made of an annular shell tightly packed with aluminum tubes of high length-to-diameter ratio, designed to maintain laminar flow in and between the tubes for all flow rates of the present tests.

The honeycomb was followed by 15 damping screens made of Monel screen soldered to annular rings of $9\frac{1}{2}$-inch inner diameter. All the screen retainers and the honeycomb shell were cut from a single piece of steel tubing and reassembled inside a section of 10-inch steel pipe which acts as a pressure shell. A large number of screens were employed to maintain a low turbulence intensity at the entrance to the test section, even though relatively large disturbances were introduced by the valves, air heaters, and elbows in the upstream flow system. The screen used was of mesh size and wire diameter such that it should not shed vortices for any available flow rate according to the data of references 12, 13, and 14. The stilling chamber and piping downstream from the heaters were covered with 4 inches of Fiberglas insulation and sealed with a coat of Insulag. This was sufficient to reduce the temperature drop between the main flow and the stilling-chamber wall to a few percent of the total temperature difference.

Velocity and temperature traverses were made at the exit plane of the stilling chamber before the initial assembly of the test section. The velocity profile was found to be flat to within less than 2 percent except in the boundary layer which extended 0.1 to 0.15 inch from the wall. The temperature profile was flat to approximately 1° F except in the boundary layer even when the most uneven heater-element combination was employed.

After the tests had been completed, an attempt was made to measure the intensity and scale of turbulence in the exit plane of the stilling chamber, but upstream of the boundary-layer suction slot. The only hot-wire anemometer equipment available was designed for application to flows of higher turbulence intensity and scale. Consequently, the actual value

of scale in the apparatus could not be measured, and the intensity measurements except in the boundary layer were almost entirely masked by the random electronic noise introduced by stray electromagnetic radiation. It was found, however, that the scale was considerably less than 0.015 inch for the range of flow rates used in the tests. The turbulence intensity $u'/\bar{U}$ in the boundary layer along the stilling-chamber wall, upstream of the boundary-layer suction slot, was found to be approximately 0.003 for low flow rates and 0.02 for flow rates corresponding to the highest used in the tests. The turbulence intensity in the core of the flow was completely masked by the random noise output on the electronic voltmeter at all flow rates. If the actual voltage due to the turbulence is taken as the order of the least count of the voltmeter (and it was apparently not larger than this), a value of $u'/\bar{U}$ of 0.0005 to 0.001 was obtained for the core.

From the stilling chamber the flow passed through the contraction nozzle. The contraction was achieved in two steps: The first from $9\frac{1}{2}$ to 3 inches and the second from 3 to $1\frac{1}{4}$ inches. Each step was designed to avoid positive pressure gradients completely, using the data of Rouse and Hassan (ref. 15).

In the second group of tests a boundary-layer suction piece (fig. 1(b)) was inserted between the stilling chamber and the contraction nozzle. It consisted of two rings of 24S-T4 aluminum machined to provide a 0.125-inch-long boundary-layer suction slot designed according to the recommendations of Loftin and Burrows (ref. 16). The suction flow was removed from the slot through 12 axially symmetric holes and was led out through equal lengths of 1/4-inch tubing to a header. From the header the suction flow was discharged to atmosphere through a standard A.S.M.E. flange-tap orifice plate and a control valve.

The test section (fig. 1(c)), which was smoothly joined to the contraction nozzle, was fabricated from a piece of seamless brass tubing 60 inches long, with a 1.25-inch inside diameter and 0.125-inch wall thickness. The test pipe had 21 wall static-pressure taps with a diameter of 0.020 inch. Except for the first few taps the spacing (see table I) was arranged to give a distance between successive taps of approximately 12 percent of the length from the inlet of the test section. The taps were located on a helix with 70° of arc between successive taps so that no two taps lay on the same axial line. All taps were made with extreme care by four stages of alternate drilling of the hole and lapping of the inside of the tube to insure freedom from burs. The test tube was finally polished bright inside.

The test section was enclosed in a tank which could be filled with water to control the test-tube wall temperature. This tank was also supplied with air jets to agitate the water and maintain uniform temperature.

The pressure taps were connected by a manifold system to a Foxboro micromanometer. The manifold system had two needle valves in series in each line and was so arranged that each pressure tap could be connected to either manifold box.

The mass flow was obtained by measuring the pressure drop across the contraction nozzle and, as a check, by measuring the pressure drop across a standard A.S.M.E. flange-tap orifice meter installed upstream of the heaters. A manometer was used to measure the total pressure in the stilling chamber, and the temperature in the stilling chamber was measured by iron-constantan thermocouples.

For the cooled runs, three thermocouples were installed in tangential slots in the tube wall and were carefully soldered over. In addition, three thermocouples were used for measuring the temperature of the contraction nozzle and of the shoulder joining the latter to the test pipe.

TEST PROCEDURES

First Group of Runs (No Boundary-Layer Suction)

Adiabatic runs.- After preliminary runs were made and the leaks had been reduced to a satisfactory level, 10 runs at various values of Re_D were made to determine the adiabatic performance of the system.

In general, measurements of pressure drop in the tube were taken in sets of three in such a way that two of them could be checked against the third. For example, measurements might be taken successively between taps 1 and 2, 2 and 3, and 1 and 3. The first two readings were then added to check against the third.

Cooled runs.- In all cooled runs a warmup period of approximately 4 hours preceded testing. During this time temperature readings were recorded approximately every half hour and the various controls adjusted. The air temperature was maintained constant at a value of approximately 325° F.

Despite the radial slots cut in the small end of the contraction nozzle to serve as heat-flux barriers, it was found initially that end conduction from the test section lowered the temperature of the inner wall of the contraction nozzle to a value about midway between that of the cooling water and that of the air stream. To eliminate this temperature differential, electrical heaters were installed on the contraction nozzle, each controlled through a separate Variac. These Variacs were trimmed to maintain the contraction nozzle at essentially air-stream temperature.

When thermal equilibrium had been reached with a given flow rate, supply pressure, and supply temperature, three complete sets of data were taken, each with a different wall temperature. The three wall temperatures were obtained by filling the tank surrounding the test section successively with hot water, air, and cold water.

When water was used as a coolant, a trickle of air was bubbled through as a stirring device. To check that the agitation associated with this stirring did not effect transition, the air was turned on and off several times and measurements were repeated at points near the end of the laminar zone. This was done in several runs and with amounts of stirring considerably greater than normally used. No shift in the transition point was found.

Second Group of Runs (Boundary-Layer Suction)

In the second group of runs all procedures were the same as described for the first group; but, in addition, the flow through the boundary-layer suction slot was held constant in each run.

Accuracy of Results

The following table presents the percentage accuracy of the results in terms of uncertainty intervals based on 20-to-1 odds. This means that the odds are 20 to 1 against the percent error in any one value of a result exceeding the stated percentage. For example, the odds are 20 to 1 that the error in any one value of Re_x near the entrance at low flows does not exceed 3 percent. The uncertainty intervals given below have been found from a combination of statistics and judgement, and they should be regarded as best estimates rather than absolute values. A more complete description of this method of error analysis is given by Kline and McClintock (ref. 17).

Result	Uncertainty interval for 20-to-1 odds as a percent of results for which specified			
	Low flow rates		High flow rates	
	Near entrance	Near exit	Near entrance	Near exit
Re_x	3	2	3	1
$4f_{APP}$	5	2	5	2
$4f_{APP}(Re_D)$	6	3	6	2
$\frac{\bar{x}/D}{Re_D}$	3	2	3	1

EFFECT OF COOLING ON TRANSITION

Behavior of Flow in Entrance Zone of Smooth Round Tubes at High Reynolds Numbers

Shapiro and Smith (ref. 18), investigating the local apparent friction factor in the entrance section of smooth round tubes, found a zone near the entrance where the boundary layer was laminar and where the general behavior was like that on a flat plate. The laminar zone, in which the local apparent friction factor varied inversely with the square root of the length Reynolds number, extended to length Reynolds numbers between 100,000 and 500,000. After a rapid increase through the transition region, the local apparent friction factor then decreased again (approximately inversely with the one-fifth power of Re_x) in the turbulent entry zone and, as the velocity profile became stationary, finally approached the Kármán-Nikuradse friction factor for fully developed turbulent pipe flow.

It should be noted here that the local apparent friction factor f_{APP} is identical with the skin-friction coefficient for fully developed pipe flow but differs from the latter near the inlet of a pipe. The velocity profile in the entrance zone of a tube changes as the flow moves down the tube, thus causing a pressure change due to the change in the momentum flux from section to section. Since the square velocity profile at the tube inlet has less momentum flux than any other profile for the same flow rate, the momentum changes in the entrance section cause a drop in pressure over and above that due to skin friction. The local apparent friction factor, defined by the equation

$$-4f_{APP} \equiv \frac{dp/d(x/D)}{\frac{1}{2}\rho V^2}$$

is the sum of the pressure drops due to momentum change and to skin friction. It is always greater than the skin-friction coefficient in the laminar entrance zone.

In the experiments reported here, the Reynolds numbers at the transition point for adiabatic flow varied from 400,000 to over 3,750,000. This large variation was due (1) to the change in the disturbance level of the stream as the flow was altered, (2) to certain modifications that were made between the first and second groups of runs, and (3) to the use of boundary-layer suction in the second group of runs. The distinction between the first and second groups of runs is that the joints in the contraction nozzle were further lapped and the boundary-layer suction apparatus was added between the two groups of runs. In the first group

of runs no boundary-layer suction was used; in the second group of runs several constant values of boundary-layer suction flow were employed. Since the adiabatic performance of the system was not the same in the first and second groups of runs, it is necessary to describe the two groups of runs separately. In the following discussion the adiabatic performance of the first group and then of the second group of runs will be described. This will be followed by a discussion of the results obtained in the comparable cooled runs.

Adiabatic Performance

First group of runs (no boundary-layer suction).- The adiabatic characteristics of the system for the first group of runs with no boundary-layer suction are shown in figures 2(a) to 2(c). These are all logarithmic plots of apparent friction factor against free-stream Reynolds number. The points shown in these plots were computed from the data as described in appendix A.

The point where transition begins is taken to be the point at which the data deviate appreciably from a straight line with a slope of approximately -1/2. In figure 2(a) it will be seen that this point occurs between 475,000 and 550,000 and increases as the diameter Reynolds number decreases. In figure 2(b) the transition Reynolds number varies from 1,600,000 to something greater than 2,300,000, again increasing with decreasing diameter Reynolds number.

All the adiabatic data from the first group of runs are shown in figure 2(c). This figure clearly shows a sudden jump in the value of the transition Reynolds number occurring at a diameter Reynolds number of about 65,000. At this same flow rate an audible pulsation with a frequency of approximately 2 cycles per second occurred in the flow and could also be observed on the manometers. For all flow rates below that of pulsation the transition Reynolds number was of the order of 2×10^6; for all flow rates at or above that of pulsation the transition Reynolds number was of the order of 5×10^5. The sudden decrease in the transition Reynolds number with increasing flow was attributed to some portion of the tunnel system upstream of the test pipe reaching a critical Reynolds number at which vortices were shed or the boundary layer became turbulent. This would in turn produce an increase in disturbance level at the tube entrance and a consequent decrease in the transition Reynolds number.

It is believed that the pulsation observed was caused by a phenomenon similar to that which accounts for the well-known "spurting-jet" experiment, namely, that in a certain range of supply pressure there is no steady flow possible because the change from a laminar to a turbulent boundary layer may produce a discontinuity in the curve of head loss against flow for the system.

The change in the flow regime described above allowed tests of the effects of cooling at what amounts to different levels of disturbance in the tunnel.

Second group of runs (boundary-layer suction).- The second group of runs was undertaken to determine whether the effects of cooling on transition had been masked in the first group of runs owing to the presence of a slight thermal boundary layer and to an unduly high initial disturbance level in the boundary layer. For this purpose the boundary-layer suction apparatus described previously was constructed and installed. In the required disassembly it was found that some oil residue and dirt had accumulated on the spacer retaining the screen rings just ahead of the contraction nozzle. It was also noticed that a discoloration had occurred in one zone just behind the joint of the test tube to the contraction nozzle and that the converging portions of the nozzle had accumulated a thin film of sludge and very fine dirt particles. All of this dirt was removed. In addition, both joints in the contraction nozzle were further lapped. The entire contraction nozzle and test section were then polished bright on the inside. At the end of this operation neither joint could be found by touch.

The adiabatic performance of the system during the second group of runs is shown in figures 3, 4(a), and 4(b). The behavior of the system was found to be different for each of several ranges of flow rate. The first range extended up to a flow rate corresponding to a diameter Reynolds number of approximately 80,000. In this zone laminar flow extended down the entire length of the tube for all rates of boundary-layer suction flow. In run D-2, at a diameter Reynolds number of 78,000, it is seen from figure 3 that laminar flow extended to a Reynolds number of at least 3.75×10^6. Run D-2 was taken with special care using virtually all tap combinations to provide a check on tap performance and to obtain the best possible apparent local friction factors for the laminar entrance zone. The apparent local friction factors measured in this run are believed to be the best obtained, not only because of the care used but also because the flow rate was high enough to give very good precision of measurement in the pressure drops for all but a few points and also because there was no turbulent flow anywhere in the pipe to act as a disturbing influence.

For flow rates in the range of Reynolds number from 85,000 to 100,000 an audible pulsation again occurred in the system at a frequency of approximately 2 cycles per second if no boundary-layer suction flow was used. The pulsation persisted over a wider range of flows than that in the first group of tests.

At flow rates above the pulsation zone the transition point occurred at a length Reynolds number of approximately 700,000 when no boundary-layer suction was applied, as shown by the curves marked $Q_{suction}/Q_{test} = 0$

in figures 4(a) and 4(b). Application of boundary-layer suction in the zone of flow rates corresponding to diameter Reynolds numbers from 85,000 to 125,000 brought about a marked increase in transition Reynolds number. This effect is shown in figures 4(a) and 4(b) where the transition Reynolds number is increased from 700,000 to 1.8×10^6 by application of boundary-layer suction. In general, there is an optimum amount of boundary-layer suction flow which gives the greatest Reynolds number at the transition point; although, for any amount of suction flow greater than a certain critical amount, the change in the transition Reynolds number with variations in suction flow was not significant in this system.

In the zone of flow rates giving a pulsation with no boundary-layer suction flow, the application of any amount of flow through the boundary-layer suction slot greater than the critical amount would eliminate the pulsation in the main flow entirely. In the zone of flow rates greater than that at which pulsations occur, but less than that for a diameter Reynolds number of 125,000, application of increasing amounts of boundary-layer suction flow would first cause no change, then would bring about a pulsation, and finally would eliminate the pulsation again. This series of events was accompanied in each case by an increase in the transition Reynolds number from approximately 700,000 to 2,000,000. This is a good verification of the theory proposed previously to explain the sudden jump in the transition Reynolds number encountered in the first group of tests.

Demarcation of transition point.- In examining figures 2 to 4, it will be noticed that in some instances the friction factor first deviates downward from the laminar line before increasing to the turbulent value. In other instances it first rises. The downward deviation is undoubtedly due to the momentum decrease associated with the onset of transition. This belief is strengthened by the fact that the downward dip is always more pronounced for those runs where the transition Reynolds number is higher. For these cases the boundary layer would be thicker, and a change in the velocity profile within the boundary layer from a laminar type to a turbulent type would produce a greater decrease in momentum flux and thus would tend to produce a greater decrease in the apparent friction factor.

The transition point in the present tests has been taken as the point where the apparent friction factor deviates from the straight line of laminar flow either upward or downward on the logarithmic plots of $4f_{APP}$ against Re_x. This point is hard to determine exactly because of the uncertainty in the data and of the finite number of taps. Observation of the figures will show, however, that the onset of transition is defined in most cases to within 10 or at most 20 percent. To be technically significant as a means for controlling transition, cooling would have to delay transition to the extent that the Reynolds number at the beginning of transition in the cooled case was at least $1\frac{1}{2}$ or 2 times the value which occurred in the comparable adiabatic flow. An uncertainty

in Re_x of even 20 percent is, therefore, satisfactory for the present purpose.

Results for Cooled Runs

The results of the first group of runs, without boundary-layer suction, are shown in figures 5(a) to 5(j). The results of the second group of runs, with boundary-layer suction, are shown in figures 6(a) to 6(d). Each graph shows a series of runs with all variables held constant but wall temperature. All the data are presented in two ways. For the first group of runs figures 5(a) to 5(e) are logarithmic plots of local apparent friction factor against free-stream Reynolds number, while figures 5(f) to 5(j) are logarithmic plots of the same data showing local apparent friction factor against mean boundary-layer Reynolds number. Similarly, for the second group of runs figures 6(c) and 6(d) show the same data as figures 6(a) and 6(d) but figures 6(c) and 6(d) are plotted on the basis of mean boundary-layer Reynolds number instead of free-stream Reynolds number.

The graphs shown in figures 5 and 6 cover a range of diameter Reynolds numbers from 50,000 to 106,000 and include cases showing Reynolds numbers at the transition point in the adiabatic flow from 500,000 to 1,800,000. All of these graphs show the same main results: (1) The free-stream Reynolds number of transition is not significantly changed by cooling, and (2) the mean boundary-layer Reynolds number of transition is usually increased by cooling. The maximum increase in the mean boundary-layer Reynolds number of transition is of the order 75 percent for an applied temperature difference of 270° F and a ratio of wall to stream temperature of 0.66. The increase in mean boundary-layer Reynolds number at the transition point indicates an increased stability due to cooling, as would be predicted from the calculations of Lees and Van Driest. But the temperature-viscosity relation is such that in these cases the free-stream Reynolds number of transition is not significantly changed. In a few cases it will be observed that the free-stream Reynolds number at the transition point is actually decreased slightly by cooling (e.g., fig. 6(b)).

From the design point of view the significant quantity is the free-stream Reynolds number of transition because this determines the physical location of the transition point. While cooling appears to increase slightly the boundary-layer Reynolds number of transition, the net effect on the physical location of the transition point is hardly discernible because of the compensating effect of the change in boundary-layer viscosity.

For the flow of air past a flat plate at Mach numbers between 0 and 0.5 and a ratio of wall to stream temperatures of 0.66, Lees (ref. 10) predicts an increase in the minimum free-stream Reynolds number at the

instability point of approximately 2,000 times the Reynolds number at the original instability point. For the same conditions the calculations of Van Driest (ref. 11) show an increase of approximately 30 times in the minimum value of the free-stream Reynolds number at the instability point. Since this temperature ratio and Mach number were obtained in the present tests, there is apparently little if any correlation between the calculations of Lees and Van Driest on the instability point and the behavior of the transition point found in the present tests.

In order to interpret these results more fully, the work of other experimental investigators which is now available will be summarized.

Summary of Other Data - Effect of Heating and Cooling on Transition

There appear to be only two published works on the effect of cooling on transition. Scherrer (ref. 19) investigated the effect of cooling for air flow past a 20° cone at Mach numbers of 1.5 and 2.0. At a Mach number of 1.50 transition was delayed by almost 100 percent through the application of 60° F to 90° F of cooling at a ratio of wall to free-stream temperature of 1.04. For these conditions the theory of Lees (ref. 10) predicts an infinite value for the minimum Reynolds number at the instability point. At a Mach number of 2.0 Scherrer found an increase in the free-stream Reynolds number at the beginning of transition of approximately 70 percent with 40° F to 50° F of cooling and a ratio of wall to stream temperature of 0.923. Lees' theory predicts the Reynolds number at the instability point to be infinite for this case. The transition Reynolds number for adiabatic flow in these experiments was measured as 3.75×10^6.

Monaghan and Cooke (ref. 20) found an increase in transition Reynolds number, owing to cooling, of roughly 50 percent for air flow on a flat plate at a Mach number of 2.43, the adiabatic transition Reynolds number being 500,000. The amount of cooling supplied was again enough to give an infinite value for the Reynolds number at the instability point according to Lees' calculations.

Since these cooling data are meager, the available data on the effect of heating will also be summarized here.

Scherrer (ref. 19) investigated the effect of heating on transition for flow of air past a 20° cone at a Mach number of 1.53. At a total pressure of 21 pounds per square inch absolute a decrease of approximately 20 percent in transition Reynolds number was observed when the surface temperature of the cone was increased from approximately 180° F to 220° F. No comparable adiabatic data were reported, but extrapolation of their data indicates an adiabatic transition Reynolds number of the order of 1.7×10^6. At a total pressure of 14.8 pounds per square inch absolute

a decrease of approximately 10 percent was observed in the transition Reynolds number as the surface temperature was increased from 160° F to 220° F. Again no comparable adiabatic data are given, but extrapolation yields an adiabatic transition Reynolds number of roughly 1.4×10^6.

Monaghan and Cooke (ref. 20) observed the effect of heating in air on a flat plate at a Mach number of 2.43. For a ratio of wall to stream temperature of 1.37 they found a decrease in transition Reynolds number of 36 percent. At a ratio of wall to stream temperature of 1.60 they found a decrease in transition Reynolds number of 41 percent. In both cases the adiabatic transition Reynolds number was 550,000. The observed effects of heating on transition were far less than the effects predicted by the theory for the change in the point of laminar instability.

Higgins and Pappas (ref. 21) investigated the effect of heating on a flat plate in air at a Mach number of 2.40. They found a decrease of only 50 percent in the transition Reynolds number for a ratio of wall to stream temperature of 2.86, which is far less than what might be anticipated from the theory. The adiabatic transition Reynolds number was 1.25×10^6.

Liepmann and Fila (ref. 22) investigated the effect of heating for air flow on a flat plate at essentially zero Mach number. Two turbulence levels were used. At a turbulence level of $u'/\overline{U} = 0.0005$ a decrease of 28 percent in the transition Reynolds number was observed for a ratio of wall to stream temperature of 1.43. For the same ratio of wall to stream temperature and a turbulence intensity of $u'/\overline{U} = 0.0017$, a decrease of 40 percent was observed. In both cases the adiabatic transition Reynolds number was 500,000. This surprisingly low value of transition Reynolds number at these turbulence levels was attributed by the authors to the effect of transverse contamination. For this temperature ratio Lees' theory (ref. 10) predicts a decrease in the Reynolds number at the instability point of roughly 50 times and that of Van Driest (ref. 11) predicts a decrease in the Reynolds number at the instability point of approximately twelvefold.

Implications of Results

Internal flows.- The present results indicate clearly that no significant change in the Reynolds number at the transition point can be expected due to cooling in normal internal flows. In most internal flows large disturbances are present. Under these conditions cooling seems to bring about little change in the Reynolds number at the transition point.

In the present investigation the turbulence level was considerably below that normally encountered in internal flows, but no significant

effect of cooling was found. It is, of course, possible that an effect would be found in tests with still lower turbulence levels, but the difficulties involved in producing these low turbulence levels would make such tests inapplicable for almost all practical situations.

General theory of transition[1].- From the foregoing discussion of the present results and the results of other investigators two major points concerning the location of the transition point are evident: (1) The amount of disturbance present has a strong effect on the Reynolds number at the transition point; (2) heating or cooling creates a change in the transition Reynolds number in the direction indicated by the theoretical calculations, but the quantitative effect is always at least one order of magnitude less than the predicted shift in the Reynolds number of the instability point. In addition, a third point appears which is not yet convincingly proved, namely, that the percentage change in the transition Reynolds number due to a given amount of heating or cooling increases as the transition Reynolds number for adiabatic flow increases (i.e., as the initial disturbance level decreases).

In the present tests the disturbance level of the tunnel increased with increasing flow, causing a decrease in the transition Reynolds number from 3.75×10^6 to 4×10^5. This disturbance level is not a simple function of one variable but appears to depend strongly on the turbulence in the free stream and in the boundary layer of the stilling chamber as well as on the smoothness and cleanliness of the joints and pressure taps in the test section. Random external noise and random agitation of the water around the test section seemed to have little or no effect. Shapiro and Smith (ref. 18) found similar results for a tube, although the disturbance levels of their tests were apparently larger, giving a range of transition Reynolds number from 1×10^5 to 5×10^5. Similarly, on a flat plate, Schubauer and Skramstad (ref. 5), as well as many other observers, found that the transition Reynolds number could be increased by a factor of more than 40 times by reduction of the disturbances in the flow. It may be recalled that no investigators prior to Schubauer and Skramstad had found experimental evidence of Tollmien-Schlichting type oscillations, apparently because of the high disturbance levels of the early tests. In such cases, as noted by Schubauer and Skramstad, the large disturbances distort any possible measurements of Tollmien-Schlichting waves. And, since the current theory deals only with very small disturbances, there is at present no experimental or theoretical information concerning how transition is brought about when large disturbances are present in the flow except that of Taylor (ref. 23) which deals only with the effect of free-stream turbulence and is based on a supposition concerning a relation between separation and transition.

---

[1]This section was read in advance by Professor C. C. Lin who generously made several helpful suggestions.

Thus, several important questions remain unanswered. First, is the mechanism by which transition is brought about in the case of large disturbances the same as that when only vanishingly small disturbances are present? This is more or less the same as asking whether the nonlinear terms of the differential equation behave in the same fashion as the linear terms which have already been investigated theoretically. Secondly, if the mechanism is essentially the same for large disturbances as for small, is the zone in which large disturbances are amplified the same as that for small disturbances?

These questions are related to the question of metastability of a given profile as opposed to complete stability. A known example of a metastable behavior is that of Poisseuille flow. Many experiments have established the following facts concerning Poisseuille flow. For all diameter Reynolds numbers less than approximately 2,000 the Poisseuille profile is completely stable, returning to laminar flow even if greatly disturbed. For diameter Reynolds numbers above 2,000 the flow is generally said to be "unstable." But the actual value of diameter Reynolds number to which laminar flow persists depends strongly on the level of disturbance present, the diameter Reynolds number of transition seeming to increase continually as the amount of disturbance is decreased. Such a condition would more properly be referred to as metastable, inasmuch as theoretical studies of the stability of the Poisseuille profile in the presence of vanishingly small disturbances have thus far failed to show an instability.

Admittedly, no proper conclusions regarding the flat-plate transition can logically be drawn by analogy to the Poisseuille case, since from the point of view of stability the two flows are quite different. However, there remains the possibility that a similar situation regarding metastability exists on a flat plate; and it is entirely conceivable that a small, yet sufficiently large, disturbance can cause transition on a flat plate by a mechanism unrelated to the present small-disturbance theory.

Another question remaining unanswered by the present theory is the interaction of various disturbances in causing transition. That such effects can be important was demonstrated by Liepmann (ref. 7) who showed that the superposition of a relatively small amount of noise, which by itself would have had a small effect, was sufficient to cause a large effect on transition at the trailing edge of a single bump.

The present results on the effect of cooling on transition, as well as the results of other investigators summarized above, tend to emphasize the incomplete state of the present knowledge on this subject. This is particularly true with regard to the possibility of other mechanisms of transition apart from that which has been so well demonstrated by the

theoretical work of Tollmien, Schlichting, Lin, and other investigators and the experimental work of Schubauer and Skramstad and of Liepmann.

It should be kept in mind that the present results do not mean that the current theory of instability is necessarily in error. But the results of calculations concerning the instability point must be applied with extreme caution, if at all, to the prediction of transition. However, the present results coupled with the results of other investigators do indicate that considerable further study is needed, particularly on the subject of nonlinear effects and other possible mechanisms of transition. The importance of such study is emphasized by the three unanswered questions discussed above. It will be noted that each of these questions is concerned with an essentially nonlinear effect, and it is unlikely that stability theory can be used to any marked extent in predicting transition until at least qualitative answers are available to all three of these questions.

Finally, it should be mentioned that the present results may not be exactly applicable to a flat plate for the following reasons:

(a) There is a favorable pressure gradient in the tube, which in itself is stabilizing. Quite possibly the stabilizing effects of cooling might be smaller in the case of a favorable pressure gradient than in the case of zero pressure gradient.

(b) There are some three-dimensional (axisymmetric) effects in the tube. These effects are believed to be very small in the present tests because the range of variables was such that the boundary-layer thickness was very small compared with the pipe radius.

(c) Because of convection currents owing to temperature gradients, there may have been slight departures from conditions of axial symmetry in the present experiments. Such a three-dimensional effect would almost certainly have a destabilizing influence. Until further experiments are performed, the significance of this factor can only be speculated on.

LOCAL APPARENT FRICTION FACTOR IN LAMINAR ENTRANCE ZONE OF SMOOTH ROUND TUBES

Review of Existing Theories

The present results convincingly demonstrate that the hypothesis of Shapiro and Smith (ref. 18) concerning the establishment of a laminar boundary layer and its subsequent transition to a turbulent layer in the entrance of a tube at high Reynolds numbers is correct. The present

results also show that this laminar layer can, by reduction of the disturbance level, be extended to considerably greater Reynolds numbers than would normally be expected.

There are at present several theories concerning the velocity profiles and apparent friction factors for the entrance of a tube in laminar flow. The oldest of these is by Boussinesq (ref. 24). This solution has long been known to give poor agreement with the data in the zone very near the entrance and is, therefore, of little use in the present work.

The second work, by Schiller (ref. 25), gives good agreement with the friction data but predicts entrance lengths that are somewhat too short. Schiller's solution is based on the assumption of a parabolic velocity distribution in the zone near the wall joined smoothly to a core which is unaffected by viscosity and has a constant axial velocity. This is equivalent to the assumption of a boundary layer and a mean flow correlated in such a way as to satisfy continuity. This solution should be very good near the entrance to the tube where the layer affected by viscosity is thin.

Atkinson and Goldstein (ref. 26) modified the solution of Boussinesq and joined it to a solution in the form of a series expansion at $\sigma = (x/D)/Re_D = 0.0075$.

Langhaar (ref. 27) developed a complete single mathematical theory which gives reasonable values of entrance length and velocity profiles.

In appendix B is presented a new and simple theory yielding a relation between the apparent friction factor in a tube and the skin-friction coefficient on a flat plate.

Correlation of Present Results

All of the theories mentioned above yield results which may be put in the form

$$\frac{p_i - p}{\frac{1}{2}\rho V^2} = 4\bar{f}_{APP}\left(\frac{L}{D}\right) = \phi(\sigma)$$

where ϕ denotes a functional relation. In other words, the pressure drop from the entrance to any other point depends only on the combined parameter Re_x/Re_D^2, rather than on the individual parameters Re_x and Re_D. A plot of $4\bar{f}_{APP}(L/D)$ against σ should thus yield a correlation of the mean apparent friction factor for all tubes at all flow rates.

In the case of the local apparent friction factor a different generalized correlation may be obtained from the foregoing relation. Since

$$4\bar{f}_{APP}\left(\frac{L}{D}\right) \equiv \int_0^{L/D} 4f_{APP}\, d\left(\frac{x}{D}\right)$$

it follows by differentiation that

$$4f_{APP} = \frac{d}{d(x/D)}\left[4\bar{f}_{APP}\left(\frac{L}{D}\right)\right]$$

Then, differentiating the relation

$$4\bar{f}_{APP}\left(\frac{L}{D}\right) \equiv \phi(\sigma) \equiv \phi\left(\frac{x/D}{Re_D}\right)$$

and noting that Re_D is constant during differentiation with respect to x/D, one gets

$$4f_{APP} = \frac{d}{d(x/D)}\left[\phi(\sigma)\right] = \frac{d}{d(x/D)}\left[\phi\left(\frac{x/D}{Re_D}\right)\right] = \frac{1}{Re_D}\,\phi'(\sigma)$$

A plot of $\left(4f_{APP}\right)Re_D$ against σ should therefore correlate all the local apparent friction factors.

In figure 7(a) all of the adiabatic data in the laminar zone are plotted in this manner. It is seen that all the data lie within ±7 percent and that 95 percent of the data lie within ±5 percent of the line given by the expression $\left(Re_D\right)4f_{APP} = 6.87/\sqrt{\sigma}$. This 5-percent scatter is what would be predicted from the uncertainty interval given in the table in the section "Accuracy of Results." In figure 22(a) the open points, representing the runs at high diameter Reynolds numbers, and the closed points, representing the runs at lower diameter Reynolds numbers correlate equally well. The method of correlation, therefore, appears to be satisfactory, but it must be tested over a wider range of diameter Reynolds numbers before it can be finally accepted.

A further check on the correlation is shown in figure 7(b) in which the mean line of the data given by $\left(Re_D\right)4f_{APP} = 6.87/\sqrt{\sigma}$ is compared with the present theory and with that of Schiller as well as with the

points from run D-2 and with the data of Shapiro and Smith (ref. 18). There is good agreement throughout.

It will be noted from figures 5(f) to 5(j), 6(c), and 6(d) that the adiabatic and the cooled data for the local apparent friction factor in the laminar zone can be correlated on a single line by the use of the mean boundary-layer Reynolds number, whereas the use of the free-stream Reynolds number produces sizable deviations between the adiabatic and cooled data as shown by figures 5(a) to 5(e), 6(a), and 6(b). The use of the arithmetic mean of the temperature as a base for the boundary-layer Reynolds number appears therefore to give entirely adequate correlation of the cooled and adiabatic data. The correlation $4f_{APP}(Re_D) = 6.87/\sqrt{\sigma}$ for the local apparent friction factor can thus be used when the stream is cooled if the Reynolds number is based on the properties at the arithmetic mean of stream and wall temperatures. It will probably apply with reasonable accuracy to heating as well.

In order to compare the results shown in figure 7(b) with the theories of Atkinson and Goldstein, of Langhaar, and with the complete theory of Schiller, the equations in figure 7(b) were integrated analytically. The results of these integrations together with the other theories are shown in figure 8 as a plot of $4\bar{f}_{APP}(L/D)$ against σ. It is seen that all the theories except that of Langhaar agree well with the integrated extrapolation of the data up to $\sigma = 0.005$. For larger values of σ the theories of Schiller, of Atkinson and Goldstein, and of Langhaar gradually curve away from the straight line representing small values of σ and approach as an asymptote the straight line with slope equal to unity marked "Poisseuille flow."

Figure 8 shows that the laminar flow through a tube can well be thought of as passing through three zones, roughly demarcated by $0 \leqq \sigma \leqq 0.005$, by $0.005 \leqq \sigma \leqq 0.1$, and by $\sigma \geqq 0.1$. In the first zone the flow behaves essentially like that on a flat plate with a boundary layer which is thin compared with the tube radius. In the second zone a gradual shift occurs as the boundary layer reaches the axis of the tube. The third zone is the well-known Poisseuille flow (fully developed laminar pipe flow). All the present data for the laminar entrance zone lie well within the first zone as can be seen in figure 7(a). The behavior of the boundary layer in the present tests is thus essentially like that on a flat plate.

CONCLUSIONS

From an experimental investigation of the effect of cooling on friction and on boundary-layer transition in the steady flow of air in the entrance of a smooth round tube, the following conclusions are indicated:

1. The amount of turbulence present in the free stream and in the boundary layer, as well as the smoothness and cleanliness of the walls, has a strong effect on the transition Reynolds number in internal flows. Smaller disturbances give higher transition Reynolds numbers.

2. Cooling apparently has little or no effect on the transition Reynolds number in normal internal flows of air (which contain comparatively large disturbances). No significant effect of cooling on transition has been found even for disturbance levels giving adiabatic transition Reynolds numbers as high as 1.8×10^6.

3. The effect of cooling or heating on the transition Reynolds number appears to be greater when the disturbances in the flow are smaller. A significant effect of cooling on transition might conceivably be found in an internal flow if the disturbance level was reduced sufficiently to give an adiabatic transition Reynolds number greater than 2×10^6. But even if such an effect could be found, the difficulties associated with the production of such a disturbance level would make the use of cooling to control transition in internal flows unfeasible for most practical applications.

4. In general, the evidence indicates that the effect of heating or cooling on the transition Reynolds number in air is qualitatively in the direction suggested by the calculations of Lees and Van Driest concerning the Reynolds number at the instability point. But in every case the size of the effect found experimentally for the shift in the transition point is at least one order of magnitude less than the change predicted for the instability point.

5. There is no question that the destruction of the laminar profile and the onset of turbulence can be brought about by the amplification of unstable waves in cases where the disturbances in the flow are sufficiently small. The present results suggest that this mechanism may well be modified or even supplanted by another as the cause of transition when any but vanishingly small disturbances are present in the flow.

6. The explanation of Shapiro and Smith concerning the existence of a laminar boundary layer for a short distance from the entrance of smooth tubes even at diameter Reynolds numbers much higher than 2,000 has been verified.

7. A correlation of the local apparent friction factor f_{APP} in the laminar entrance zone can be obtained by plotting $4f_{APP}(Re_D)$ against σ, where Re_D is the diameter Reynolds number and σ is a dimensionless parameter given by $\sigma = (x/D)/Re_D$. For $\sigma \leq 0.005$ the mean line of the present data is given by $4f_{APP}(Re_D) = 6.87/\sqrt{\sigma}$. This is in good agreement with the theory for the laminar entrance zone given herein which

yields $4f_{APP}(Re_D) = 7.15/\sqrt{\sigma}$ and with the approximate formula of Schiller, $4f_{APP}(Re_D) = 7.30/\sqrt{\sigma}$.

8. Comparison of the data with the theories of Langhaar, of Atkinson and Goldstein, and with the complete theory of Schiller shows that the formula $4f_{APP}(Re_D) = 6.87/\sqrt{\sigma}$ cannot hold for $\sigma \geqq 5 \times 10^{-3}$. It also shows that laminar flow in tubes can well be thought of as divided into three zones: For $\sigma \leqq 0.005$ the flow behaves essentially like that along a flat plate; for $0.005 \leqq \sigma \leqq 0.1$ the flow alters as the Poisseuille velocity profile is established; for $\sigma \geqq 0.1$ steady Poisseuille flow is maintained.

Massachusetts Institute of Technology,
Cambridge, Mass., September 30, 1952.

APPENDIX A

ANALYSIS OF DATA

Discussion

Since no velocity exceeded 200 feet per second in any of the tests, the flow was treated as incompressible.

The data for a given run were corrected to the basis of a standard flow rate and standard properties which were selected to be in the middle of the range for the given test.

Flow coefficient of contraction nozzle.- The flow coefficient of the contraction nozzle was computed as a function of diameter Reynolds number by the method of Shapiro and Smith (ref. 18). The calculated flow coefficient for the contraction nozzle is compared in figure 9 with the flow coefficient recommended by the A.S.M.E. The method of calculation is given in the section "Calculation of flow coefficient for contraction nozzle."

Boundary-layer growth in contraction nozzle.- The effective entrance point of the tube to be used in determining the values of the length Reynolds number is subject to question, since some boundary layer builds up in the contraction nozzle. The effective length of the nozzle was analyzed both on a one-dimensional basis and by plotting of the early adiabatic data for slope and minimum scatter. These considerations indicated that this effective length was not more than 1.2 inches and not less than 0.8 inch. With this in mind, the value of 1.00 inch was adopted for the effective length of the nozzle to the first pressure tap. The latter was located 1/16 inch downstream of the end of the curved nozzle contour.

Proper mean location between pressure taps.- In the method of measurement used in these tests the local apparent friction factor was not measured at a point but over some finite distance Δx. It was therefore necessary either to differentiate the curve of p against x or to calculate the appropriate distance $\bar{x}$ at which to plot a given value of friction factor deduced from the ratio $\Delta p/\Delta x$. The latter method was employed throughout.

A good approximation for the proper value $\bar{x}$ in the laminar entrance zone of a tube, for $\sigma \leq 0.005$, is the average of the arithmetic and geometric mean values of the distance rrom the entrance of the tube to the two taps used. A proof of this statement is given later. The difference between this value of $\bar{x}$ and the simple arithmetic mean of the distances to the taps from the tube entrance is small unless the ratio

of the two distances is large. A graph of the percentage correction to the arithmetic mean is shown in figure 10, from which it is seen that the proper mean distance $\bar{x}$ does not deviate from the arithmetic mean by 1 percent until the ratio of the distances to the two taps from the tube entrance exceeds 1.33.

In the transition and turbulent zones the ratio of the two values of x between successive taps was always so near unity that the arithmetic mean value for $\bar{x}$ was used with the certainty that no appreciable error was involved.

Development of Computing Equations

Calculation of flow coefficient for contraction nozzle.- For steady incompressible flow between the stilling chamber and the first pressure tap in the pipe, one may write

$$\frac{V_o^2}{2g} + \frac{p_o}{\rho g} = \frac{p_1}{\rho g} + \frac{V_1^2}{2g} + H_L \tag{A1}$$

where subscript o refers to the stilling chamber and subscript 1 to conditions at the first tap. By continuity,

$$\left(\frac{V_o}{V_1}\right)^2 = \left(\frac{d_o}{d_1}\right)^4 = \frac{1}{3,350}$$

where d_o and d_1 are the diameters of the stilling chamber and test section at the first tap, respectively, and thus it is possible to neglect the term $V_o^2/2g$ in equation (A1). Hence,

$$p_o - p_1 = \frac{\rho V_1^2}{2} + \rho g H_L \tag{A2}$$

From the definition of $4\bar{f}_{APP}$,

$$H_L \equiv 4\bar{f}_{APP}\left(\frac{L}{D}\right)\frac{V_1^2}{2g} \tag{A3}$$

Then, combining equations (A2) and (A3), there is obtained:

$$p_o - p_1 = \frac{\rho V_1^2}{2}\left[1 + 4\bar{f}_{APP}\left(\frac{L}{D}\right)\right]$$

or

$$V_1 = \sqrt{\frac{1}{1 + 4\bar{f}_{APP}\left(\frac{L}{D}\right)}}\sqrt{\frac{2(p_o - p_1)}{\rho}} \tag{A4}$$

The flow coefficient C_D of the nozzle is defined by

$$V_1 \equiv C_D\sqrt{\frac{2(p_o - p_1)}{\rho}} \tag{A5}$$

Comparison of equations (A4) and (A5) then shows that

$$C_D = \frac{1}{\sqrt{1 + 4\bar{f}_{APP}\left(\frac{L}{D}\right)}} \tag{A6}$$

The values of the flow coefficient for the contraction nozzle shown in figure 9 were obtained by use of equation (A6). The values of $4\bar{f}_{APP}(L/D)$ used for this purpose were obtained from the integrated form of the present theory in the form

$$4\bar{f}_{APP}\left(\frac{L}{D}\right) = 14.30\sqrt{\sigma} \tag{A7}$$

and the value of L for the nozzle up to the first pressure tap was taken to be 1.00 inch as explained above. These values of $4\bar{f}_{APP}(L/D)$ agree with the mean line of the data to 4 percent and the L of the nozzle is known to approximately 15 percent. The uncertainty in the value of the flow coefficient due to these possible errors, however, is at most only 0.3 percent because of the form of equation (A6).

Calculation of Re_{x_1} and Re_{x_2}.- Using the curve of figure 9 for the flow coefficient of the contraction nozzle together with equation (A5), the free-stream Reynolds number can be found as:

$$Re_{x_1} \equiv \frac{\rho_o V_1 \bar{x}}{\mu_o} = \frac{\bar{x}\rho_o C_D}{\mu_o}\sqrt{\frac{2(p_o - p_1)}{\rho}} \tag{A8}$$

The mean boundary-layer Reynolds number Re_{x_2} is the Reynolds number based on the free-stream and wall temperatures. Noting that $\mu = b + cT^{0.74}$ for air where b and c are constants, Re_{x_2} may be related to Re_{x_1} by the expression

$$Re_{x_2} \equiv \frac{\rho_m V_1 \bar{x}}{\mu_m} = \frac{\rho_o V_1 \bar{x}}{\mu_o} \frac{\rho_m}{\rho_o} \frac{\mu_o}{\mu_m} = Re_{x_1} \left(\frac{2T_o}{T_o + T_w} \right)^{1.74} \tag{A9}$$

Calculation of $4f_{APP}$ from test data.- The apparent friction factor $4f_{APP}$ is, by definition, expressed by

$$-4f_{APP} = \frac{\Delta p / \Delta(x/D)}{\frac{1}{2}\rho V^2}$$

Combining this with equation (A5), it is found that

$$-4f_{APP} = \frac{\Delta p / \Delta(x/D)}{C_D^2 (p_o - p_i)} = \frac{D}{C_D^2} \frac{\Delta p / \Delta x}{p_o - p_i} \tag{A10}$$

from which $4f_{APP}$ is conveniently computed from the measured data.

Proper Value of $\bar{x}$ for Laminar Flow in Entrance Zone of Tube for $\sigma \leq 5 \times 10^{-3}$

The proper value of $\bar{x}$ for plotting a local apparent friction factor measured between two taps for laminar flow in the early entrance zone of a tube is shown below to be the average of the arithmetic and geometric means of the distances of the two taps from the entrance of the tube.

For $\sigma \leq 0.005$ the local apparent friction factor can be expressed by the equation $4f_{APP}(Re_D) = 6.87/\sqrt{\sigma}$. For any one run under steady-state conditions this is of the form

$$4f_{APP} = B/\sqrt{x} \tag{A11}$$

where B is a constant for the run.

Now let x_n be the distance to the near tap and x_r the distance to the far tap. In the experiment, one measures an apparent friction factor $4f_{APP}'$ which is some kind of a mean over the distance $\Delta x = x_n - x_r$. That is,

$$4f_{APP}' = \frac{1}{x_r - x_n}\int_{x_n}^{x_r} \frac{B}{\sqrt{x}}\,dx = \frac{2B}{x_r - x_n}\left(\sqrt{x_r} - \sqrt{x_n}\right)$$

which may be rearranged in the form

$$4f_{APP}' = \frac{2B}{\sqrt{x_r} + \sqrt{x_n}} \tag{A12}$$

What is needed now is the value $\bar{x}$ at which $4f_{APP} = 4f_{APP}'$.

At a distance $\bar{x}$ from the entrance of the tube, $4f_{APP}$ is given by equation (A11) as

$$\left(4f_{APP}\right)_{x=\bar{x}} = B\Big/\sqrt{\bar{x}} \tag{A13}$$

Comparison of equations (A12) and (A13) then shows that

$$\sqrt{\bar{x}} = \frac{\sqrt{x_r} + \sqrt{x_n}}{2}$$

or

$$\bar{x} = \frac{x_r + 2\sqrt{x_r x_n} + x_n}{4} = \frac{1}{2}\left(\frac{x_r + x_n}{2} + \sqrt{x_r x_n}\right)$$

which is the result stated previously.

APPENDIX B

LAMINAR ENTRANCE THEORY

In this appendix there is presented a simple theory for the laminar entrance zone based on the integral momentum equations of the boundary layer.

Relation between f_{APP} and C_f.- Consider a control surface of width dx extending across the tube at section x as shown by the following sketch:

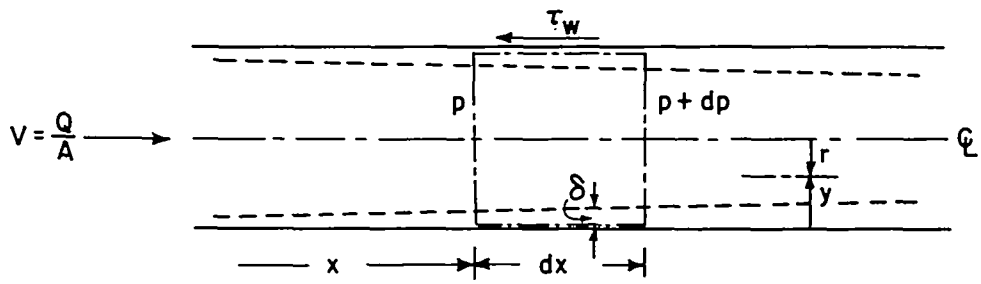

The flow is assumed to consist of a frictionless core with the speed u_c together with an annular boundary layer of thickness δ. As is usual in thin-boundary-layer theory, the pressure is taken to be uniform over each cross section. Since only the entrance region is of interest here, where the boundary layer is very thin, it is assumed that δ/D is small compared with unity. At the beginning of the tube $(x = 0)$, the velocity is assumed uniform with the value V.

The continuity equation may be written as

$$\frac{\pi D^2}{4}\rho V = \int_0^{D/2} 2\pi r\rho u \, dr$$

$$= 2\pi\int_0^{\delta} \rho u\left(\frac{D}{2} - y\right) dy + 2\pi\int_{\delta}^{D/2} \rho u_c\left(\frac{D}{2} - y\right) dy \qquad (B1)$$

The velocity distribution in the boundary layer is now assumed to be of the form

$$1 - \frac{u}{u_c} = \left(1 - \frac{y}{\delta}\right)^m \qquad (B2)$$

where m is a shape parameter independent of x.

The expression for u given by equation (B2) is now substituted into equation (B1), thus giving

$$\frac{VD^2}{4} = 2\int_0^{\delta} u_c\left[1 - \left(1 - \frac{y}{\delta}\right)^m\right]\left(\frac{D}{2} - y\right) dy + 2\int_{\delta}^{D/2} u_c\left(\frac{D}{2} - y\right) dy$$

which, to first-order terms in δ/D, may be expressed approximately as

$$\frac{VD^2}{4} = 2\int_0^{D/2} u_c\left(\frac{D}{2} - y\right) dy - 2\int_0^{\delta} u_c\left(1 - \frac{y}{\delta}\right)^m \frac{D}{2}\, dy$$

or, upon integration, as

$$\frac{V}{u_c} = 1 - \frac{4}{m + 1}\frac{\delta}{D} + \cdots \tag{B3}$$

The dynamic equation for the frictionless core may be written as

$$-dp = \rho u_c\, du_c = \rho\, d\left(u_c^2/2\right) \tag{B4}$$

By definition, the apparent friction factor is given by

$$-4f_{APP} = \frac{dp/d(x/D)}{\frac{1}{2}\rho V^2} \tag{B5}$$

Combination of equations (B4) and (B5) now yields

$$f_{APP} = \frac{1}{4}\frac{d\left(u_c/V\right)^2}{d(x/D)} \tag{B6}$$

The momentum equation for the flow through the control surface is

$$-\frac{\pi}{4}D^2\, dp - \tau_w \pi D\, dx = d\int_0^{D/2} 2\pi r \rho u^2\, dr$$

Dividing this by $\frac{1}{2}\rho V^2 \pi D\, dx$, and noting that $C_f \equiv \tau_w \Big/ \frac{1}{2}\rho V^2$, there is obtained

$$f_{APP} = C_f + \frac{4}{DV^2}\frac{d}{dx}\int_0^{D/2} u^2 r\, dr \tag{B7}$$

The integral in this expression is evaluated with the help of equation (B2) as

$$\int_0^{D/2} u^2 r\, dr = \delta\int_0^1 u_c^2\left[1 - \left(1 - \frac{y}{\delta}\right)^m\right]^2\left(\frac{D}{2} - y\right) d\left(\frac{y}{\delta}\right) + \int_\delta^{D/2} u_c^2\left(\frac{D}{2} - y\right) dy$$

Carrying out the integration, there is obtained

$$\int_0^{D/2} u^2 r\, dr = \frac{(u_c D)^2}{8} - \frac{3m + 1}{2(m + 1)(2m + 1)}\delta u_c^2 D \tag{B8}$$

whence it follows from equation (B7) that

$$f_{APP} = C_f + \frac{\frac{1}{2}\,d\left(u_c/V\right)^2}{d(x/D)} - 2\,\frac{d}{d(x/D)}\left[\frac{3m + 1}{(m + 1)(2m + 1)}\,\frac{\delta}{D}\left(\frac{u_c}{V}\right)^2\right]$$

Since m has been assumed to be independent of x, this expression may be rearranged with the help of equation (B6) as

$$f_{APP} = C_f + 2f_{APP} - \frac{2(3m + 1)}{(m + 1)(2m + 1)}\left[\left(\frac{u_c}{V}\right)^2\frac{d\delta}{dx} + \frac{\delta}{D}\,\frac{d\left(u_c/V\right)^2}{d(x/D)}\right] \tag{B9}$$

From equations (B6) and (B3) one may obtain, to first-order terms in δ/D,

$$f_{APP} = \frac{1}{4}\frac{d}{d(x/D)}\left(\frac{1}{1 - \frac{4}{m + 1}\frac{\delta}{D}}\right)^2 \approx \frac{1}{4}\frac{d}{d(x/D)}\left(1 + \frac{8}{m + 1}\frac{\delta}{D}\right)$$

or

$$f_{APP} \approx \frac{2}{m + 1}\frac{d\delta}{dx} \tag{B10}$$

Replacing $d\delta/dx$ in equation (B9) with the value given by equation (B10), and retaining only first-order terms in δ/D, there is finally obtained after rearrangement

$$f_{APP} = \left(2 + \frac{1}{m}\right)C_f \tag{B11}$$

Evaluation of m.- Equation (B11) gives a relation which depends only on the assumptions of the analysis and which is not dependent on an assumption of flat-plate-like flow. However, to choose a value of m, it is necessary to compare with a known solution. For this comparison the flat-plate solution of Blasius is used. This is equivalent to assuming that the pressure gradient in the tube has a negligible influence on the velocity profile in the zone $y \leq \delta$. In particular, m is evaluated so that the friction factors obtained are in agreement with the Blasius relation for flow past a flat plate with a velocity profile of the same form as that used above.

When the integral boundary-layer theory is applied in the usual manner to the flow on a flat plate with the velocity profile of the form of equation (B2), there is obtained

$$C_f\sqrt{Re_x} = \sqrt{\frac{2m^2}{(m + 1)(2m + 1)}} \tag{B12}$$

whereas the exact Blasius solution for the flat plate yields

$$C_f\sqrt{Re_x} = 0.664 \tag{B13}$$

Comparison of equations (B12) and (B13) then suggests that one choose the value

$$m = 1.45$$

in order to make the approximate solution identical with the exact solution.

Substituting this value of m into equation (B11), there is obtained

$$f_{APP} = 2.67C_f \tag{B14}$$

Now, combining this with equation (B13), there is obtained

$$4f_{APP} = 7.15\sqrt{Re_x} \tag{B15}$$

which may be rearranged to give

$$4f_{APP}\,Re_D = 7.15\sqrt{\sigma} \tag{B16}$$

It is interesting to note from equation (B14) that, in the laminar entrance zone, the pressure drop due to the changing momentum flux is 1.67 times as large as the pressure drop due to skin friction.

REFERENCES

1. Tollmien, W.: Über die Entstehung der Turbulenz. Nach. Gesell. Wiss. Göttingen, Math. Phys. Klasse, 1929, pp. 21-44. (Available in English translation as NACA TM 609.)

2. Tollmien, W.: Ein allgemeines Kriterium der Instabilität laminarer Geschwindigkeitsverteilungen. Nach. Gesell. Wiss. Göttingen, Math. Phys. Klasse, Neue Folge, Bd. I, Nr. 5, 1935, pp. 79-114. (Available in English translation as NACA TM 792.)

3. Schlichting, H.: Amplitudenverteilung und Energiebilanz der kleinen Störungen bei der Plattenströmung. Nach. Gesell. Wiss. Göttingen, Math. Phys. Klasse, Neue Folge, Bd. I, Nr. 4, 1935, pp. 47-78.

4. Prandtl, L.: The Mechanics of Viscous Fluids. The Development of Turbulence. Vol. III of Aerodynamic Theory, div. G, sect. 26, W. F. Durand, ed., Julius Springer (Berlin), 1935, pp. 178-190.

5. Schubauer, G. B., and Skramstad, H. K.: Laminar-Boundary-Layer Oscillations and Transition on a Flat Plate. NACA Rep. 909, 1948.

6. Liepmann, H. W.: Investigation of Boundary Layer Transition on Concave Walls. NACA WR W-87, 1945. (Formerly NACA ACR 4J28.)

7. Liepmann, H. W.: Investigations on Laminar Boundary-Layer Stability and Transition on Curved Boundaries. NACA WR W-107, 1943. (Formerly NACA ACR 3H30.)

8. Lin, C. C.: On the Stability of Two-Dimensional Parallel Flows. Part I, Quart. Appl. Math., vol. III, no. 2, July 1945, pp. 117-142; Part II, vol. III, no. 3, Oct. 1945, pp. 218-234; Part III, vol. III, no. 4, Jan. 1946, pp. 277-301.

9. Lees, Lester, and Lin, Chia Chiao: Investigation of the Stability of the Laminar Boundary Layer in a Compressible Fluid. NACA TN 1115, 1946.

10. Lees, Lester: The Stability of the Laminar Boundary Layer in a Compressible Fluid. NACA Rep. 876, 1947.

11. Van Driest, E. R.: Calculation of the Stability of the Laminar Boundary Layer in a Compressible Fluid on a Flat Plate With Heat Transfer. Rep. No. AL-1334, North American Aviation, Inc., revised Feb. 1952.

12. Dryden, Hugh L., and Schubauer, G. B.: The Use of Damping Screens for the Reduction of Wind-Tunnel Turbulence. Jour. Aero. Sci., vol. 14, no. 4, Apr. 1947, pp. 221-228.

13. Schubauer, G. B., and Spangenberg, W. G.: Effects of Screens in Wide-Angle Diffusers. NACA Rep. 949, 1949. (Supersedes NACA TN 1610.)

14. Eckert, B., and Pflüger, F.: The Resistance Coefficient of Commercial Round Wire Grids. NACA TM 1003, 1942.

15. Rouse, H., and Hassan, M. M.: Cavitation-Free Inlets and Contractions. Mech. Eng., vol. 71, no. 3, Mar. 1949, pp. 213-216.

16. Loftin, Laurence K., Jr., and Burrows, Dale L.: Investigations Relating to the Extension of Laminar Flow by Means of Boundary-Layer Suction Through Slots. NACA TN 1961, 1949.

17. Kline, S. J., and McClintock, F. A.: Describing Uncertainties in Single-Sample Experiments. Mech. Eng., vol. 75, no. 1, Jan. 1953, pp. 3-8.

18. Shapiro, Ascher H., and Smith, R. Douglas: Friction Coefficients in the Inlet Length of Smooth Round Tubes. NACA TN 1785, 1948.

19. Scherrer, Richard: Comparison of Theoretical and Experimental Heat-Transfer Characteristics of Bodies of Revolution at Supersonic Speeds. NACA Rep. 1055, 1951. (Supersedes NACA RM A8L28, TN 1975, TN 2087, TN 2131, and TN 2148.)

20. Monaghan, R. J., and Cooke, J. R.: The Measurement of Heat Transfer and Skin Friction at Supersonic Speeds. Part III - Measurements of Overall Heat Transfer and the Associated Boundary Layers on a Flat Plate at $M_1 = 2.43$. T.N. No. Aero. 2129, British R.A.E. (Farnborough), Dec. 1951.

21. Higgins, Robert W., and Pappas, Constantine C.: An Experimental Investigation of the Effect of Surface Heating on Boundary-Layer Transition on a Flat Plate in Supersonic Flow. NACA TN 2351, 1951.

22. Liepmann, Hans W., and Fila, Gertrude H.: Investigations of Effects of Surface Temperature and Single Roughness Elements on Boundary-Layer Transition. NACA Rep. 890, 1947. (Supersedes NACA TN 1196.)

23. Taylor, G. I.: Some Recent Developments in the Study of Turbulence. Proc. Fifth Int. Cong. Appl. Mech. (Sept. 1938, Cambridge, Mass.), John Wiley & Sons, Inc., 1939, pp. 294-310.

24. Boussinesq, J.: Hydrodynamique. Comp. rend., Acad. Sci. (Paris), t. 110, 1890, pp. 1160-1166, 1238-1242; t. 113, 1891, pp. 9-15, 49-51.

25. Schiller, L.: Die Entwicklung der laminaren Geschwindigkeitsverteilung und ihre Bedeutung für Zähigkeitsmessungen. Z.a.M.M., Bd. 2, Heft 2, 1922, pp. 96-106.

26. Fluid Motion Panel of the Aeronautical Research Committee and Others (S. Goldstein, ed.): Modern Developments in Fluid Dynamics. Vol. I. The Clarendon Press (Oxford), 1938, pp. 297-307.

27. Langhaar, Henry L.: Steady Flow in the Transition Length of s Straight Tube. Jour. Appl. Mech., vol. 9, no. 2, June 1942, pp. A-55 - A-58.

TABLE I

LOCATION OF PRESSURE TAPS

IN TEST SECTION

Tap	Distance from tube entrance, in.
1	1
2	2
3	3
4	4
5	5
6	6
7	7
8	8
9	9
10	11
11	13
12	16
13	19
14	23
15	27
16	31
17	35
18	41
19	47
20	53
21	59

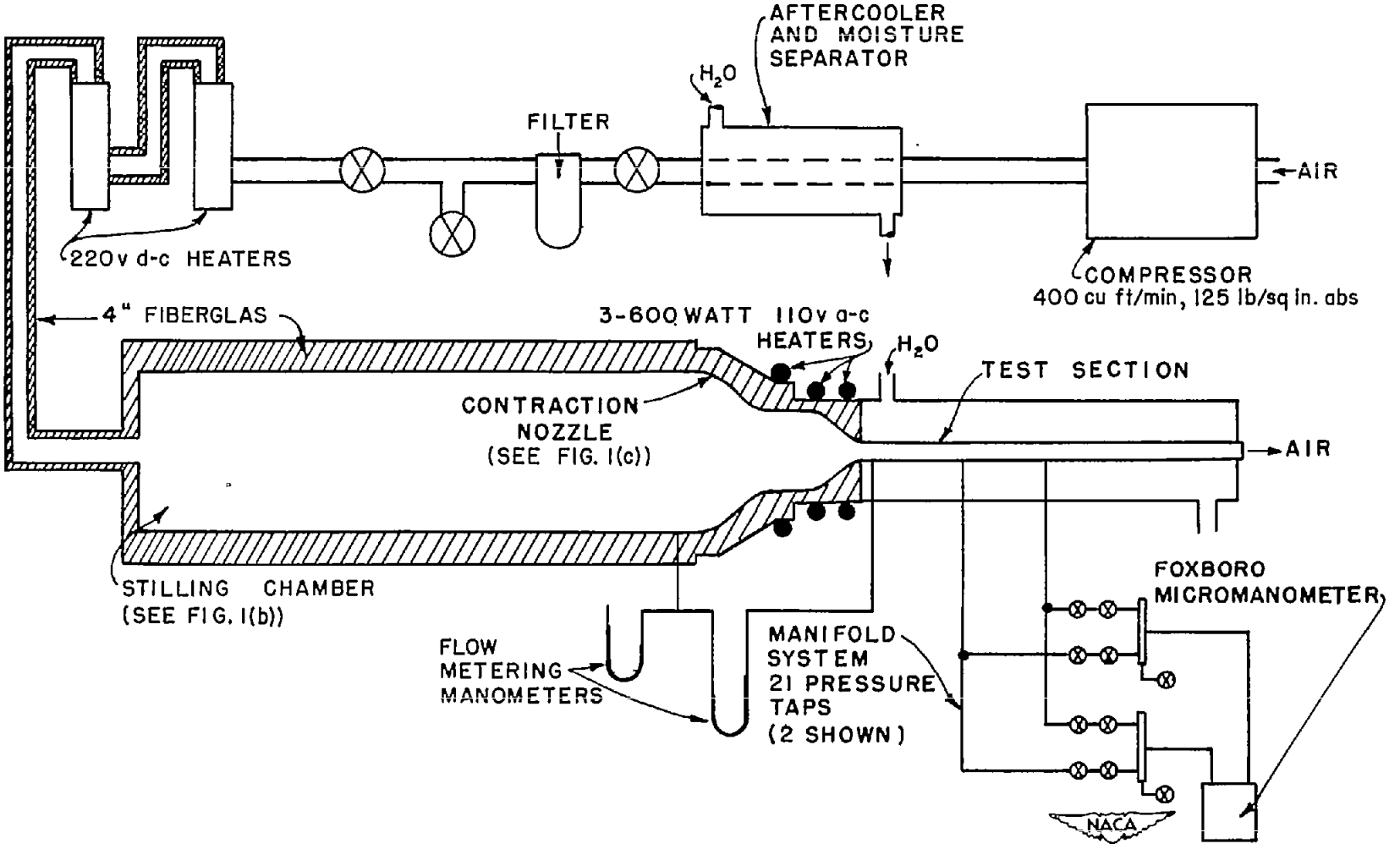

(a) Entire flow system.

Figure 1.- Schematic diagrams of test apparatus.

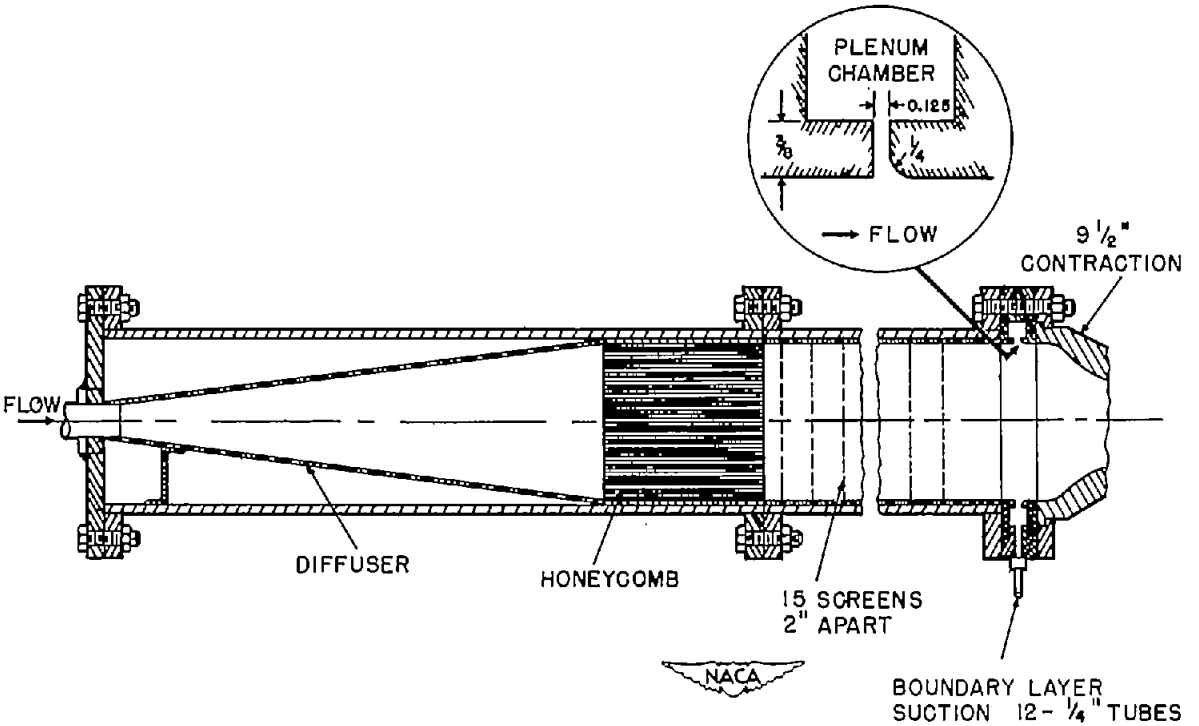

(b) Stilling chamber. Flow was straightened and smoothed by diffuser and honeycomb. Honeycomb constructed of tightly packed aluminum tubes with 0.196-inch inside diameter, 8.9 inches long, and with 0.004-inch wall thickness. Turbulence intensity was reduced by use of 15 damping screens made of square mesh Monel screen, 30 mesh per inch, 0.0065-inch-diameter wire. Boundary-layer suction apparatus had a radial slot 0.125 inch in width. Air was withdrawn from suction-slot plenum chamber through 12 holes of 21/64-inch diameter and through equal lengths of 1/4-inch tubing to header of flow control system. Boundary-layer suction apparatus used only in second group of runs.

Figure 1.- Continued.

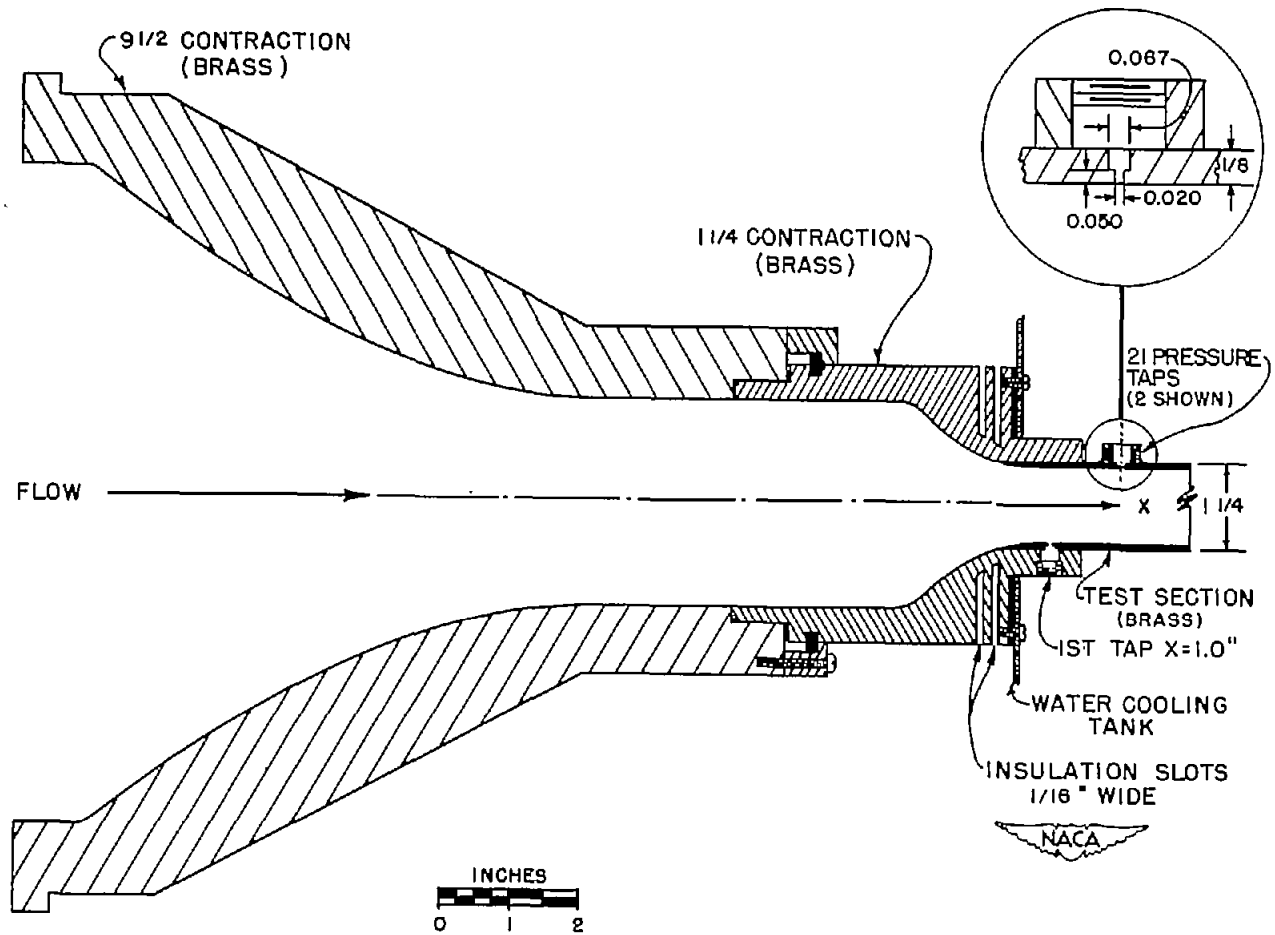

(c) Contraction nozzle and test section. All taps were constructed by four stages of drilling and lapping to remove burs. Taps were spaced on a helix with 70° of arc between successive taps so that no two taps lay on same radial line. Distances of taps from effective entrance of tube are given in table I.

Figure 1.- Concluded.

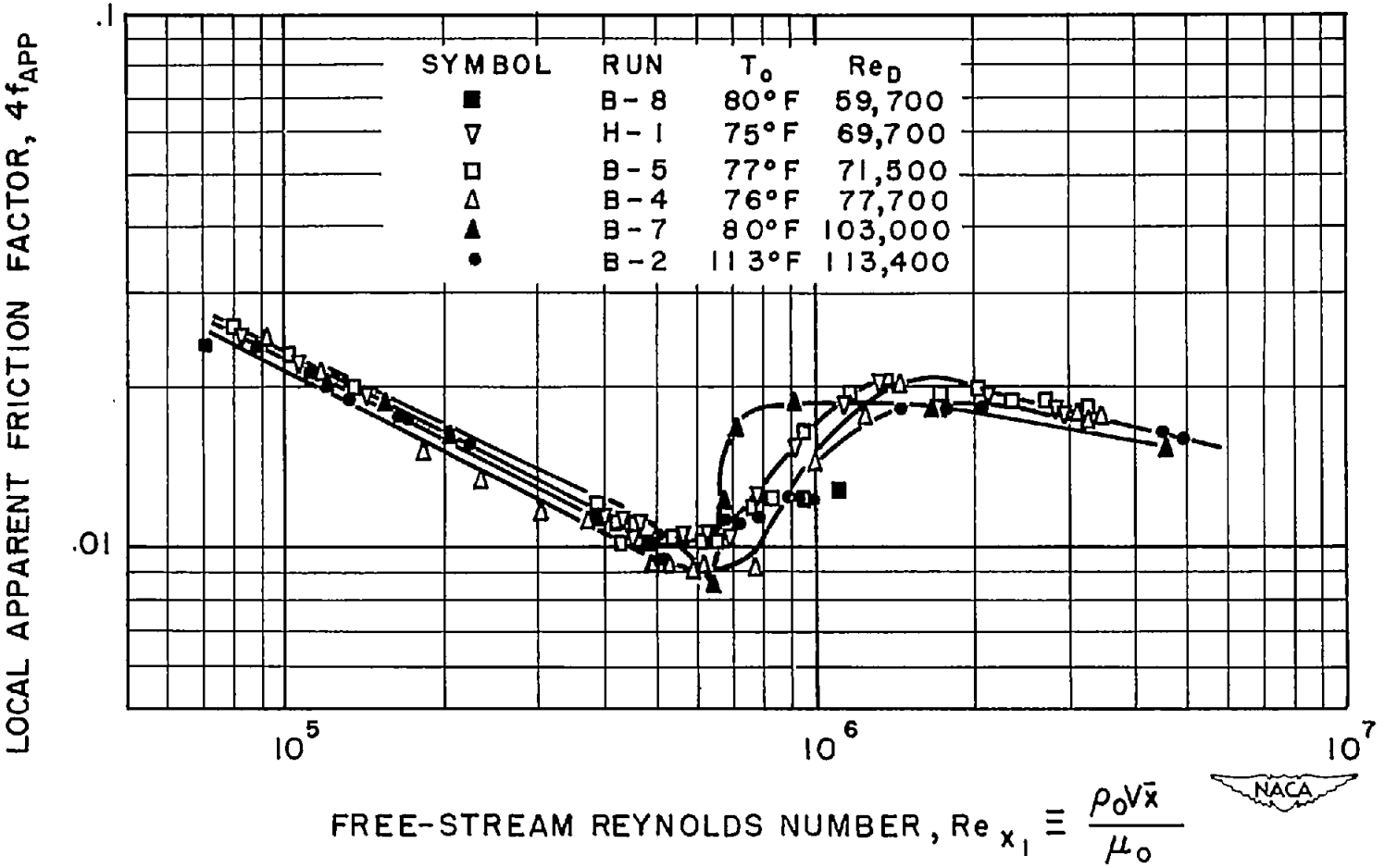

(a) For flow rates above that of pulsation.

Figure 2.- Adiabatic performance of system. First group of runs (no boundary-layer suction).

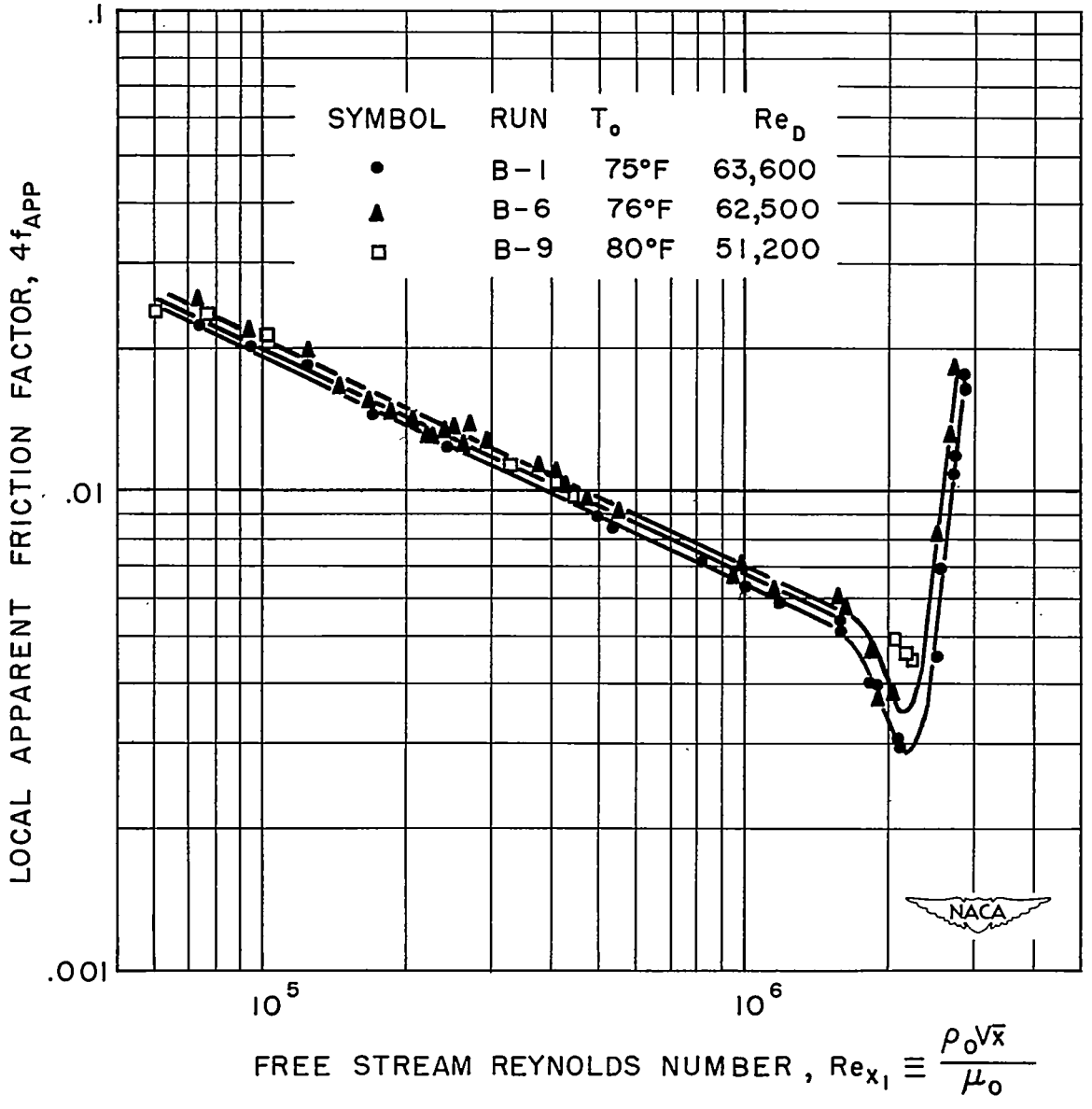

(b) For flow rates below that of pulsation.

Figure 2.- Continued.

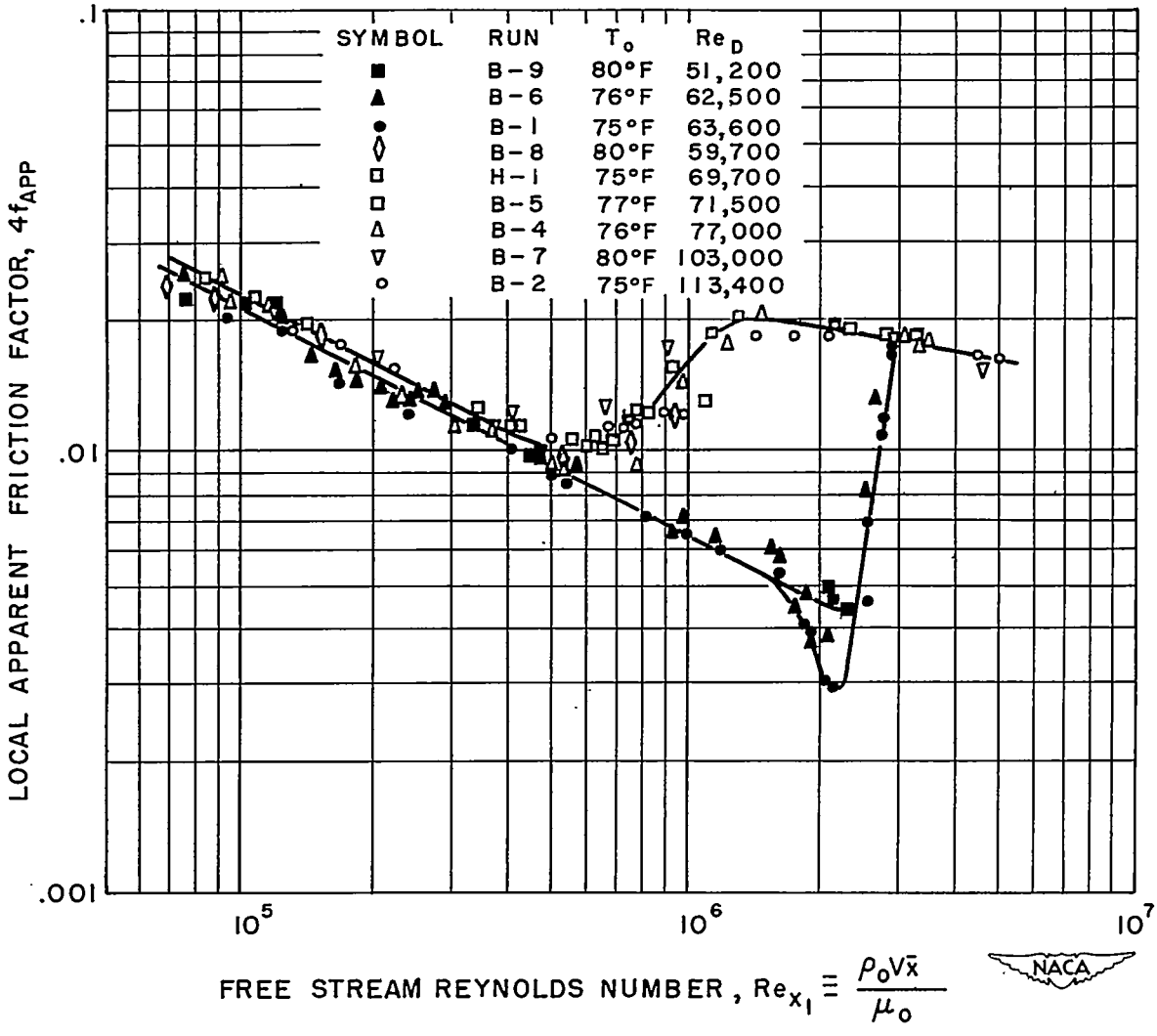

(c) For all flow rates.

Figure 2.- Concluded.

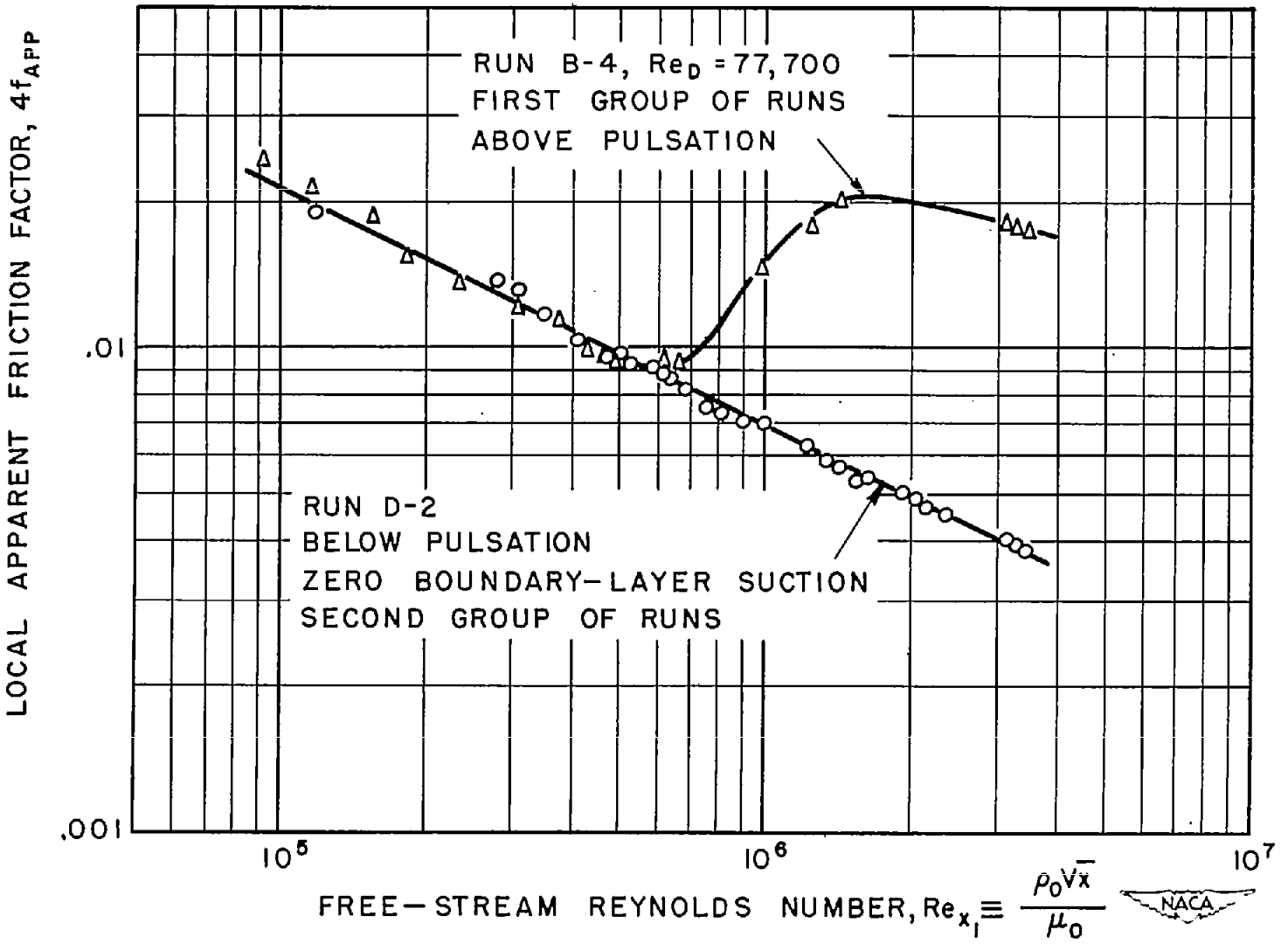

Figure 3.- Comparison of adiabatic performance of system before and after modification at $Re_D \approx 78,000$.

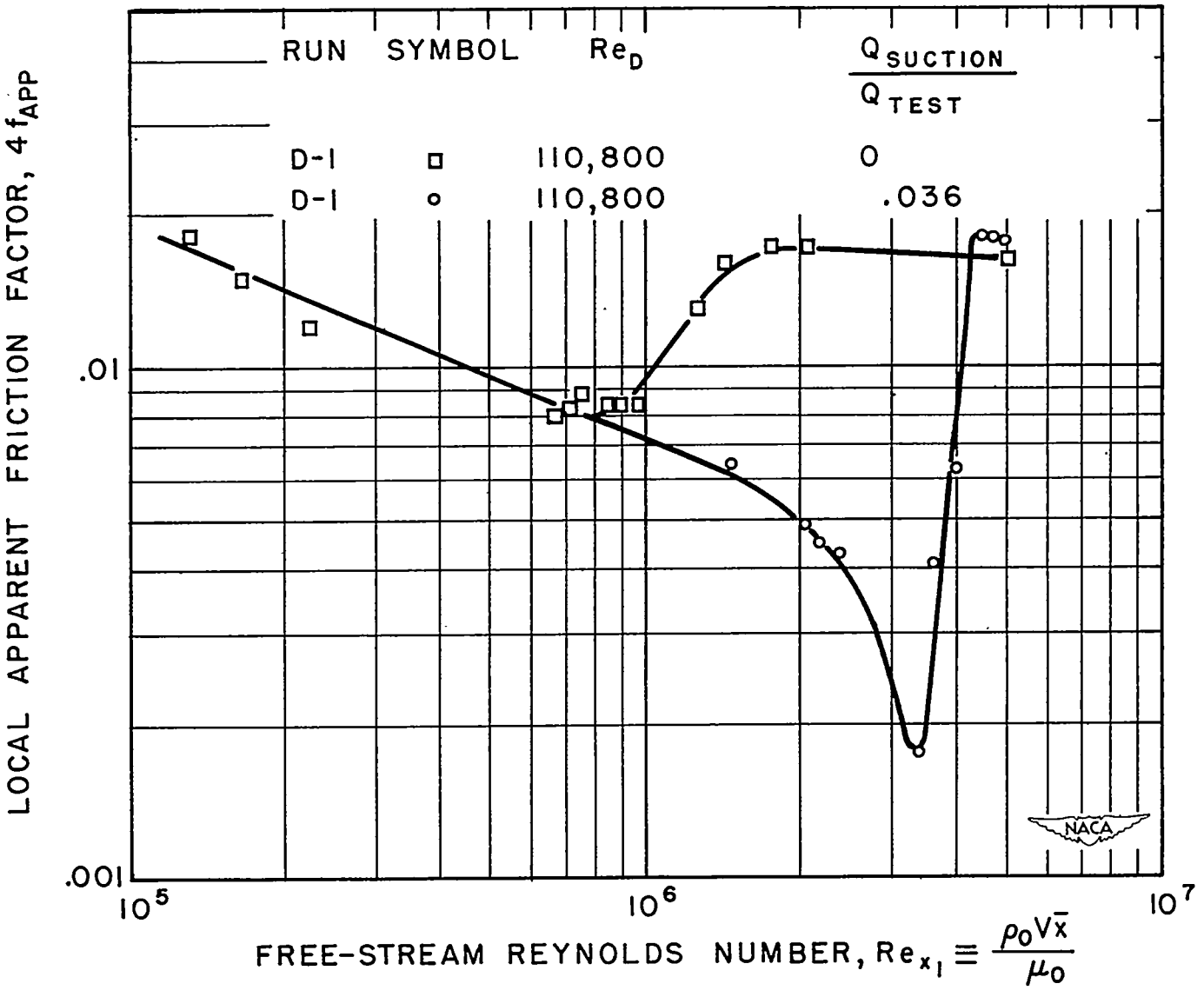

(a) $Re_D \approx 111{,}000$.

Figure 4.- Effect of boundary-layer suction on adiabatic performance of system after modification. Flow rate above pulsation; second group of runs.

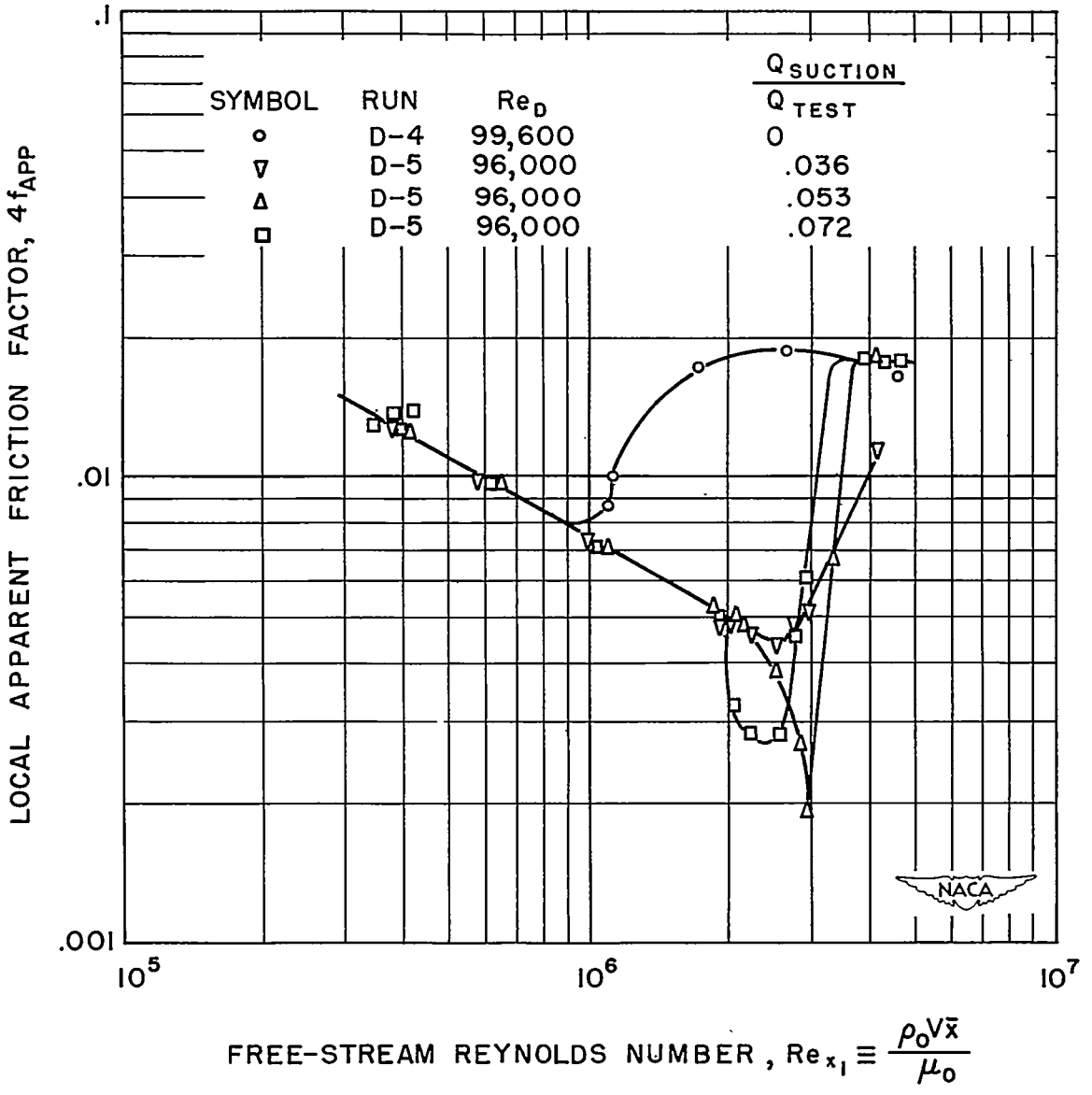

(b) $Re_D \approx 96{,}000$.

Figure 4.- Concluded.

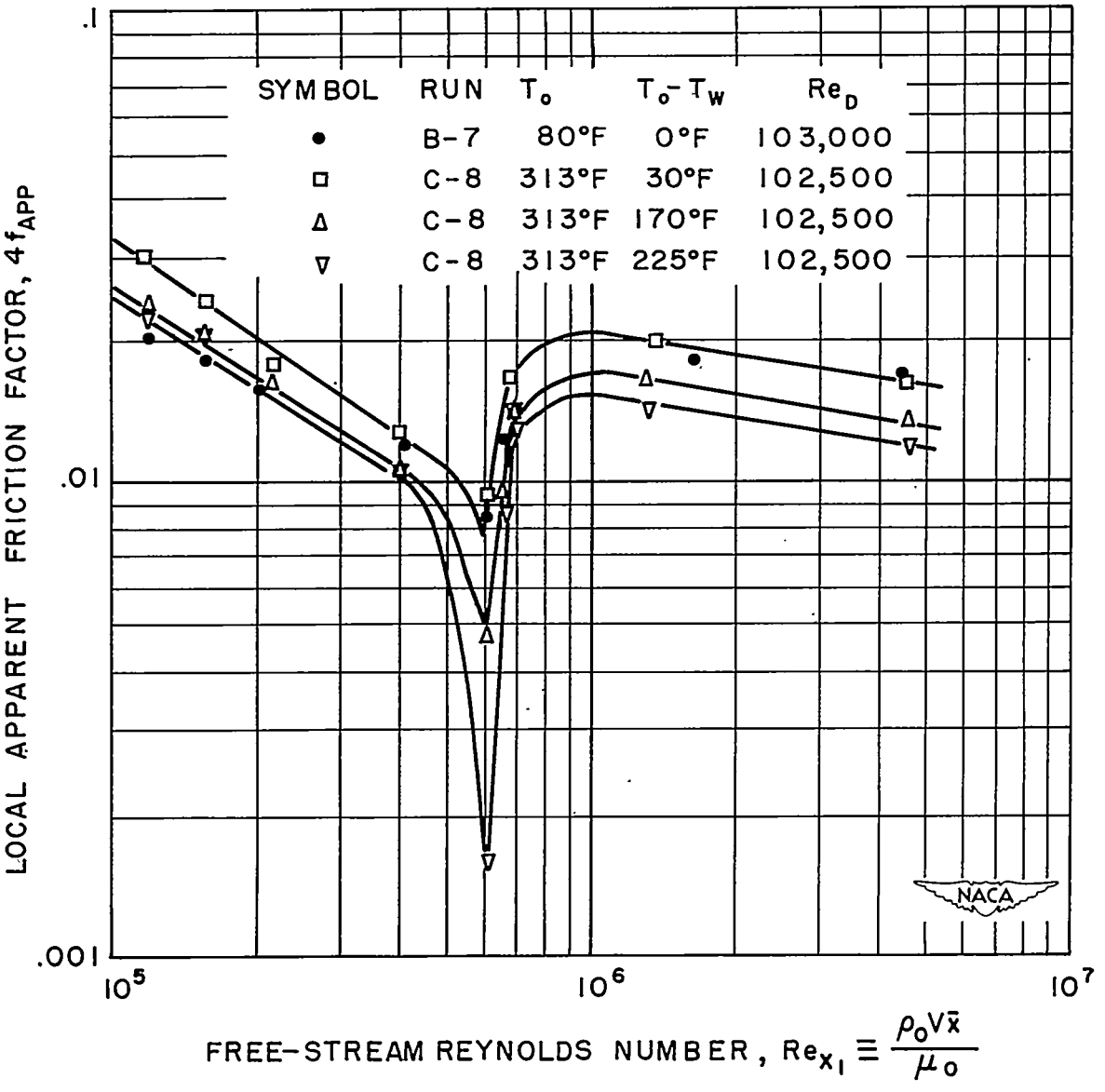

(a) Flow rate above pulsation with $Re_D \approx 102,000$.

Figure 5.- Effect of cooling on transition. First group of runs (no boundary-layer suction).

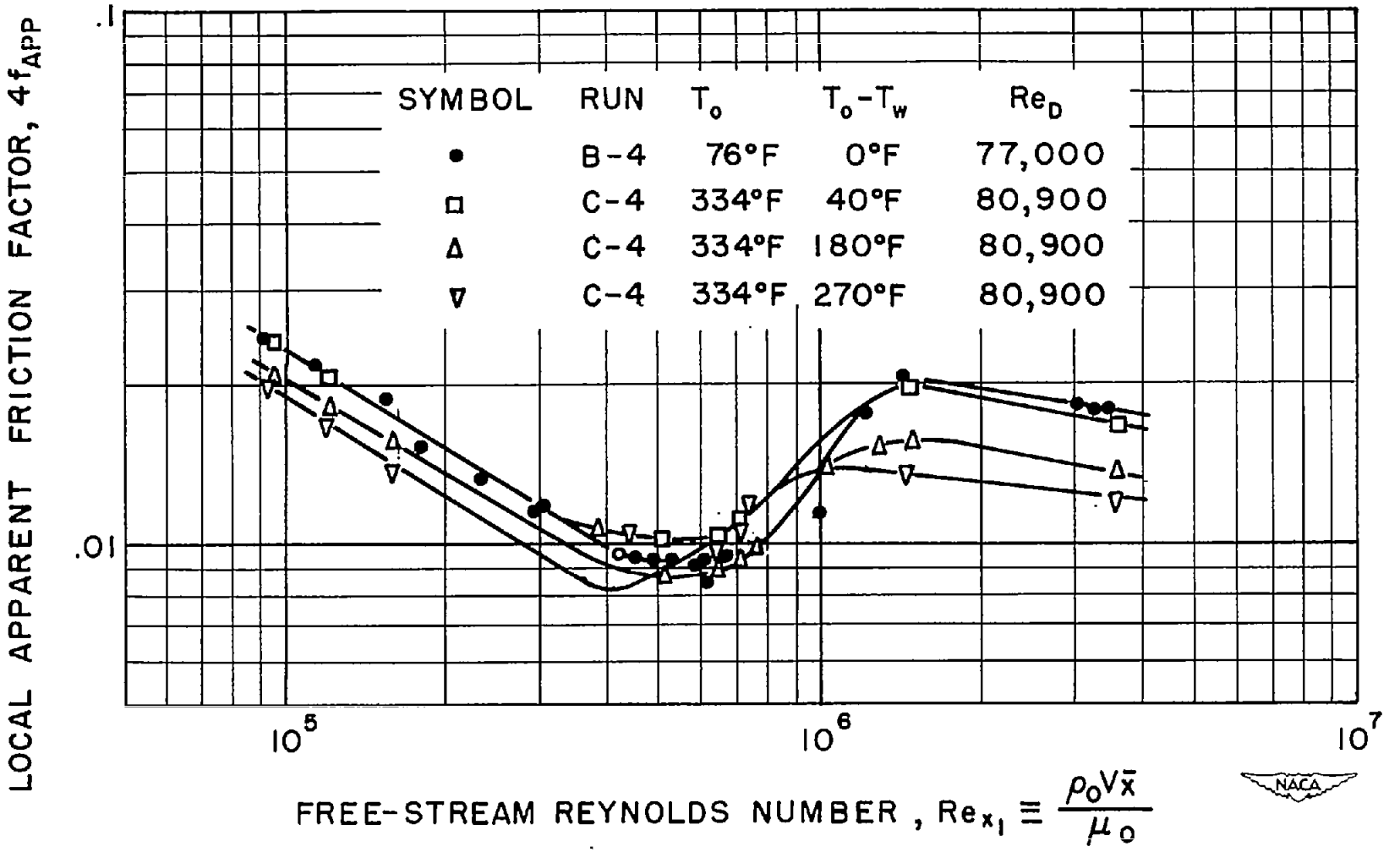

(b) Flow rate above pulsation with $Re_D \approx 79,000$.

Figure 5.- Continued.

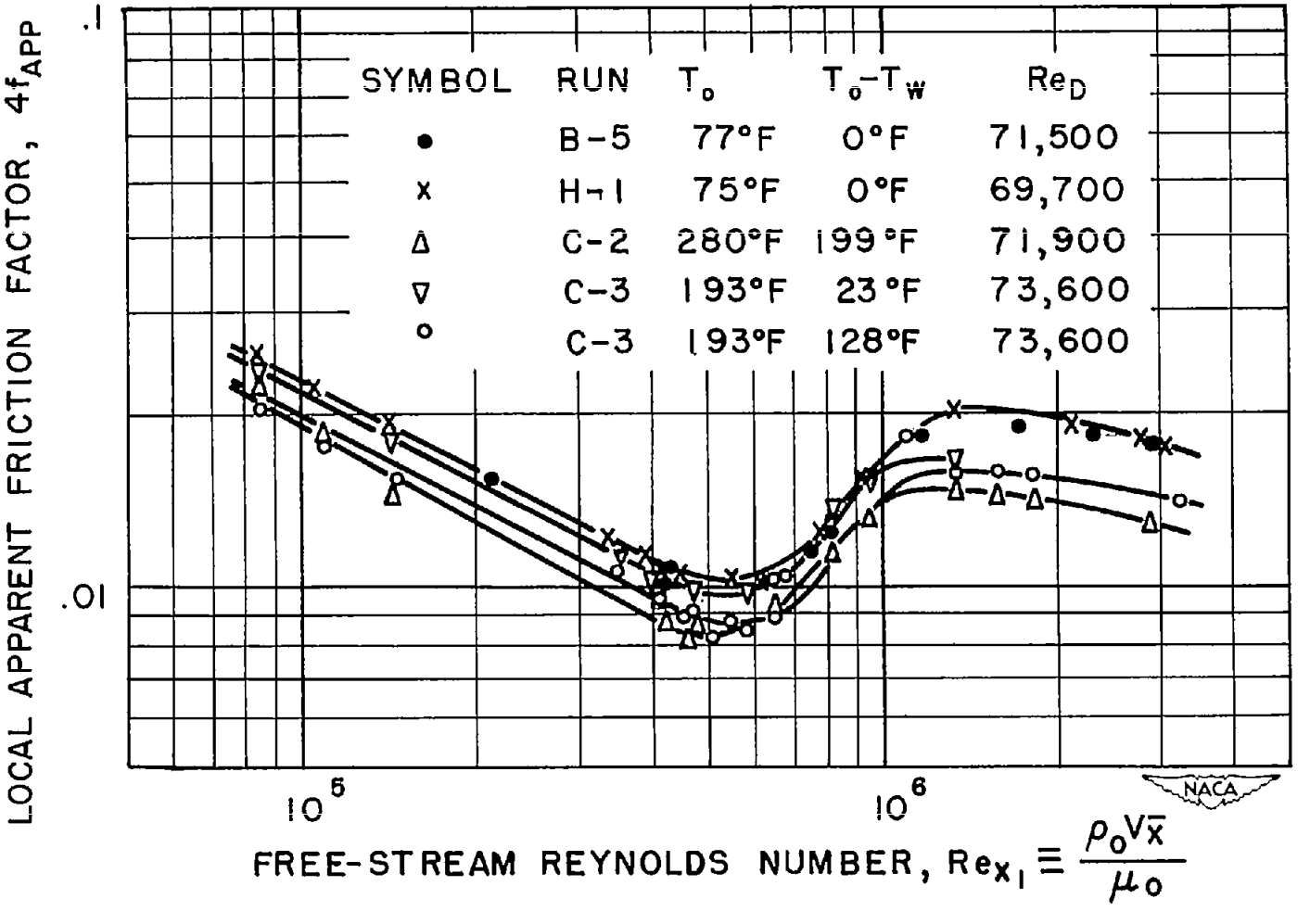

(c) Flow rate above pulsation with $Re_D \approx 70,000$.

Figure 5.- Continued.

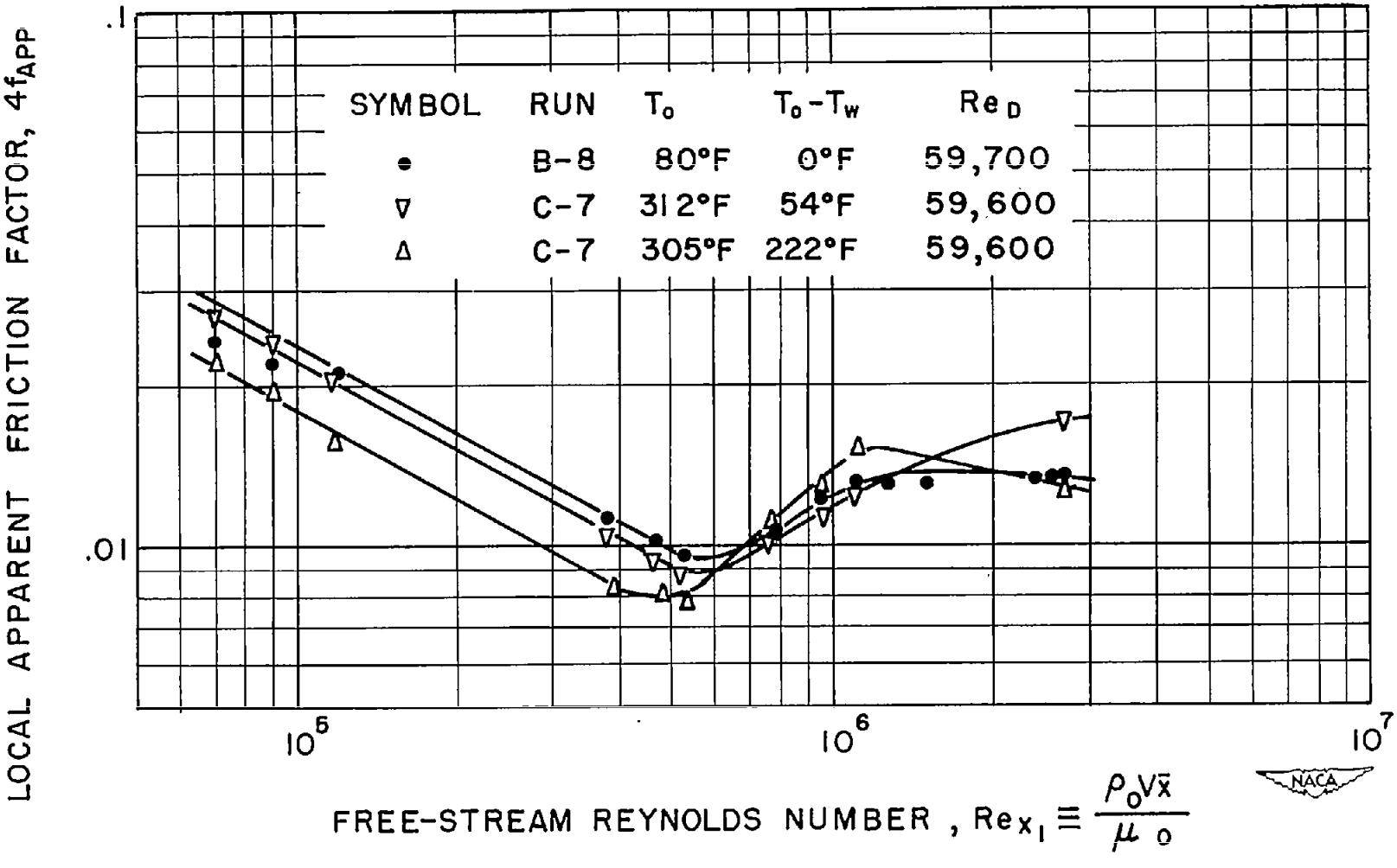

(d) Flow rate above pulsation with $Re_D \approx 60,000$.

Figure 5.- Continued.

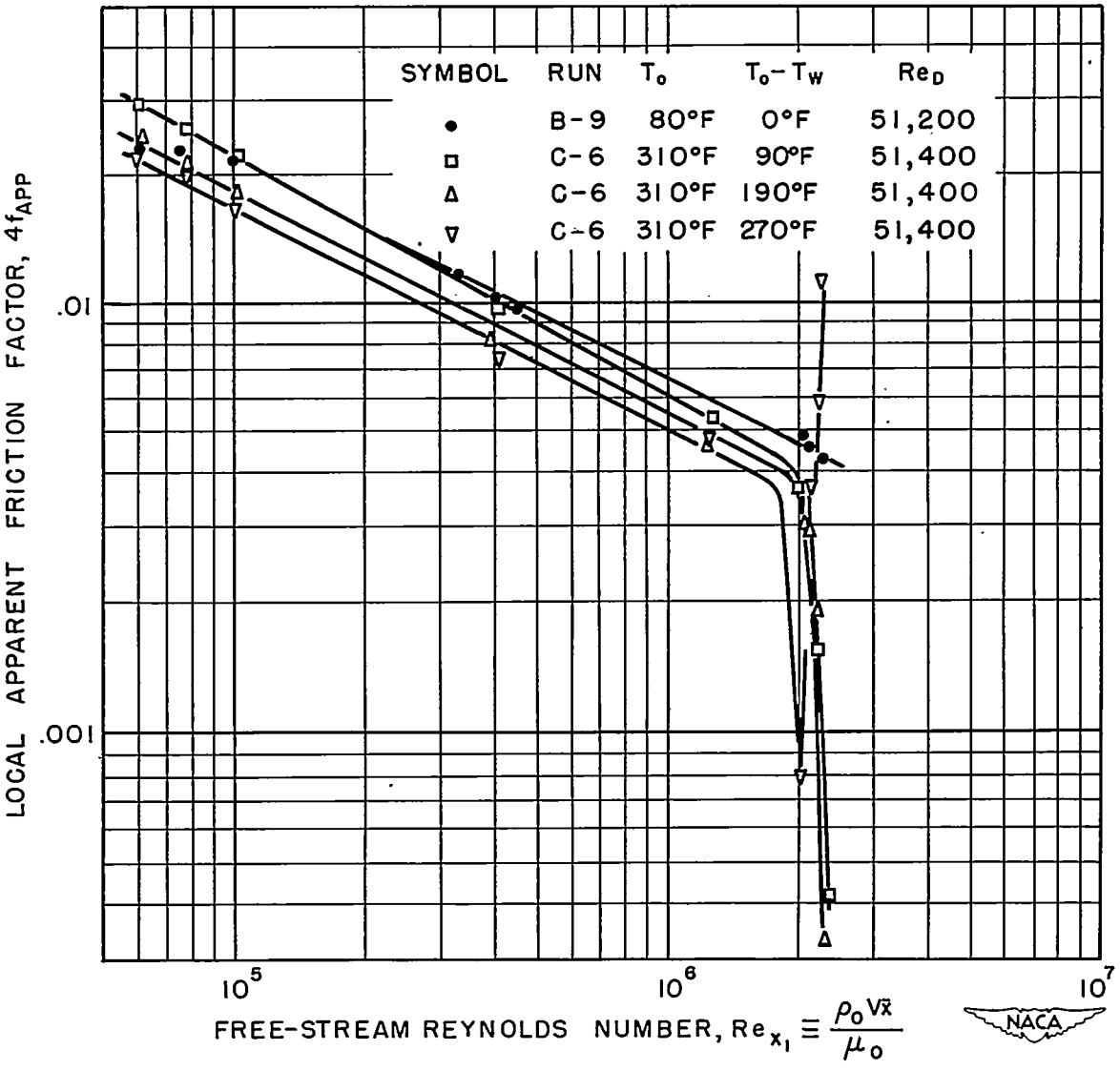

(e) Flow rate below pulsation with $Re_D \approx 51{,}000$.

Figure 5.- Continued.

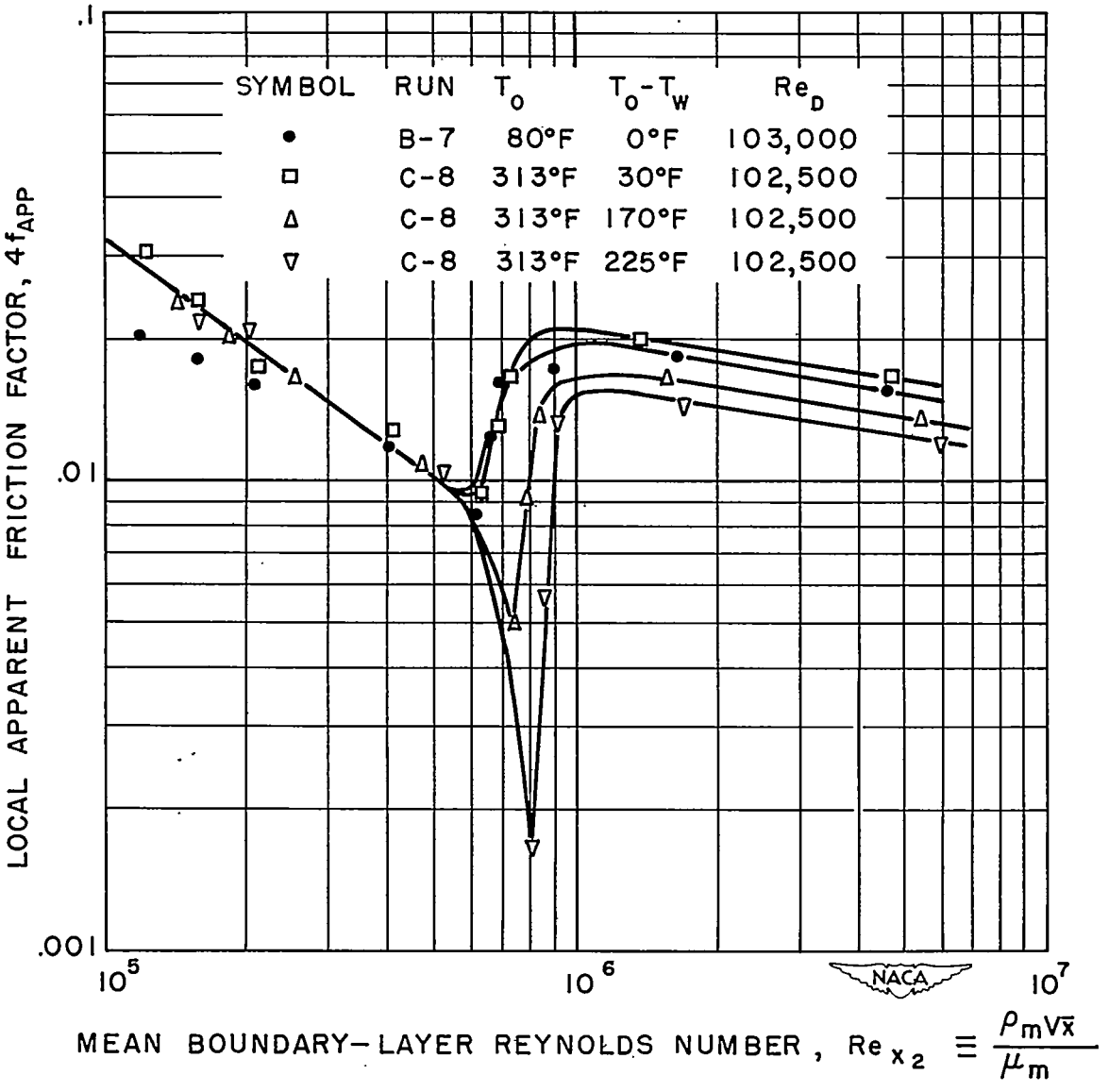

(f) Flow rate above pulsation with $Re_D \approx 102{,}000$. Same as figure 5(a) except that mean boundary-layer Reynolds number is used in place of free-stream Reynolds number.

Figure 5.- Continued.

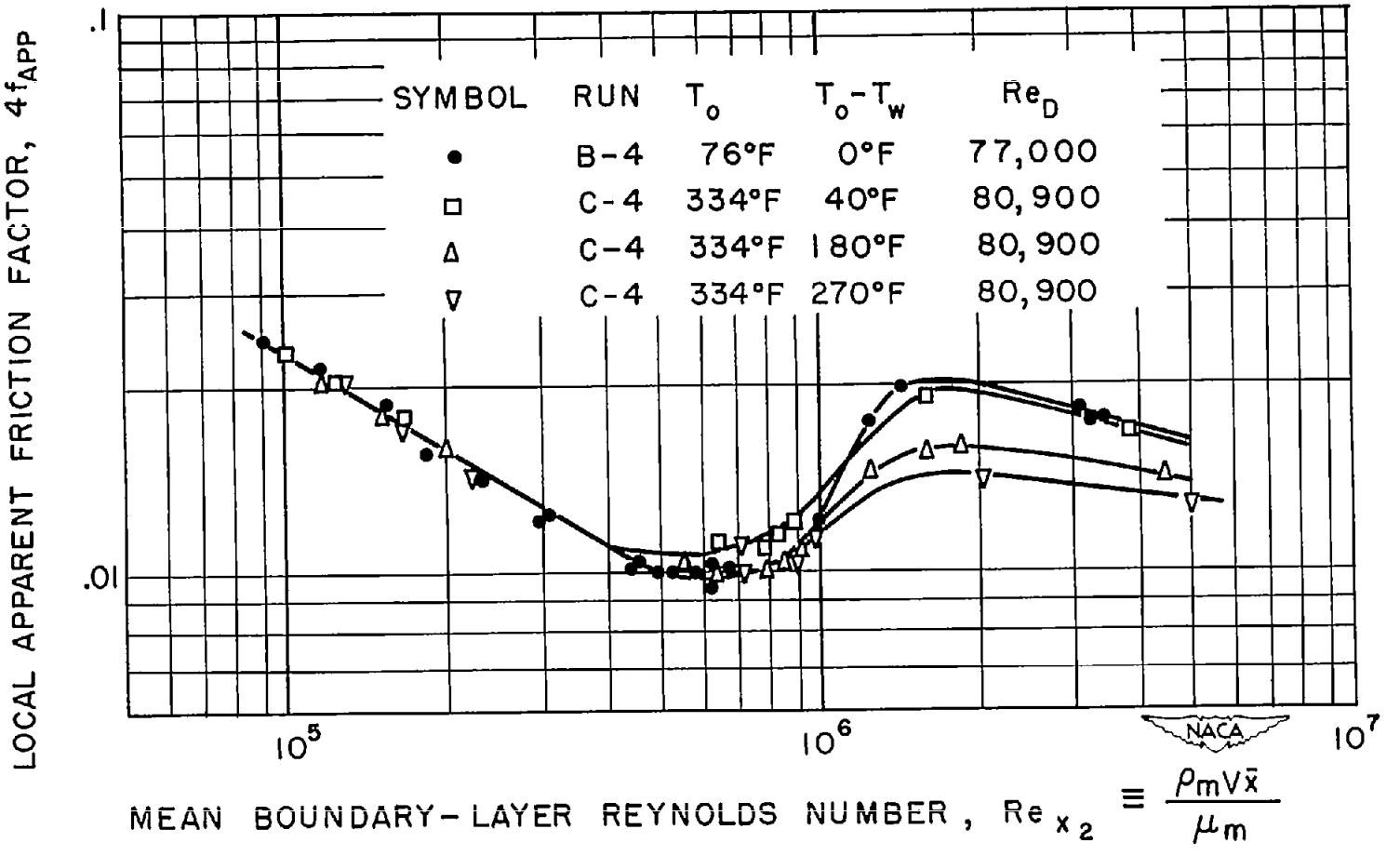

(g) Flow rate above pulsation with $Re_D \approx 79,000$. Same as figure 5(b) except that mean boundary-layer Reynolds number is used in place of free-stream Reynolds number.

Figure 5.- Continued.

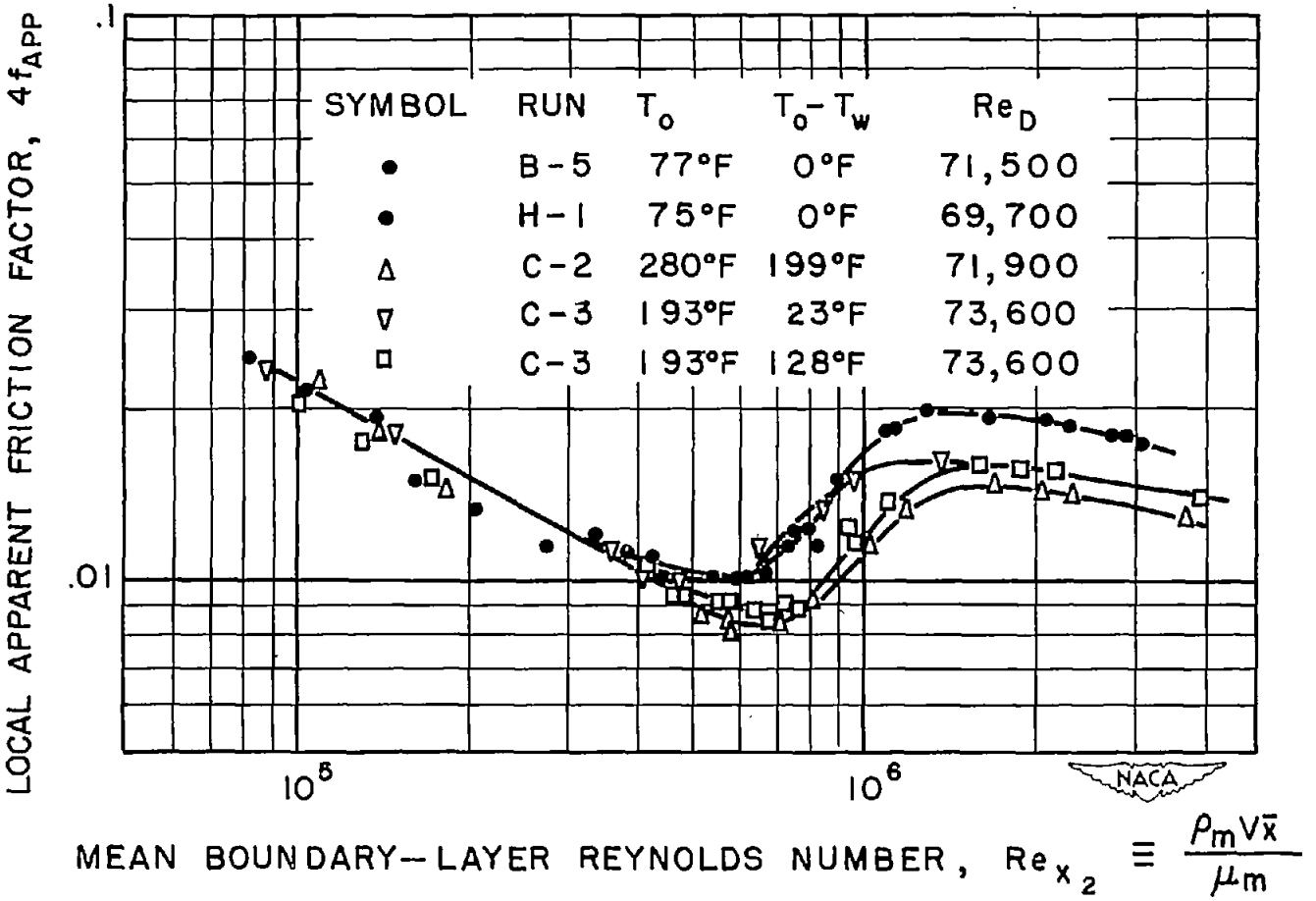

(h) Flow rate above pulsation with $Re_D \approx 70{,}000$. Same as figure 5(c) except that mean boundary-layer Reynolds number is used in place of free-stream Reynolds number.

Figure 5.- Continued.

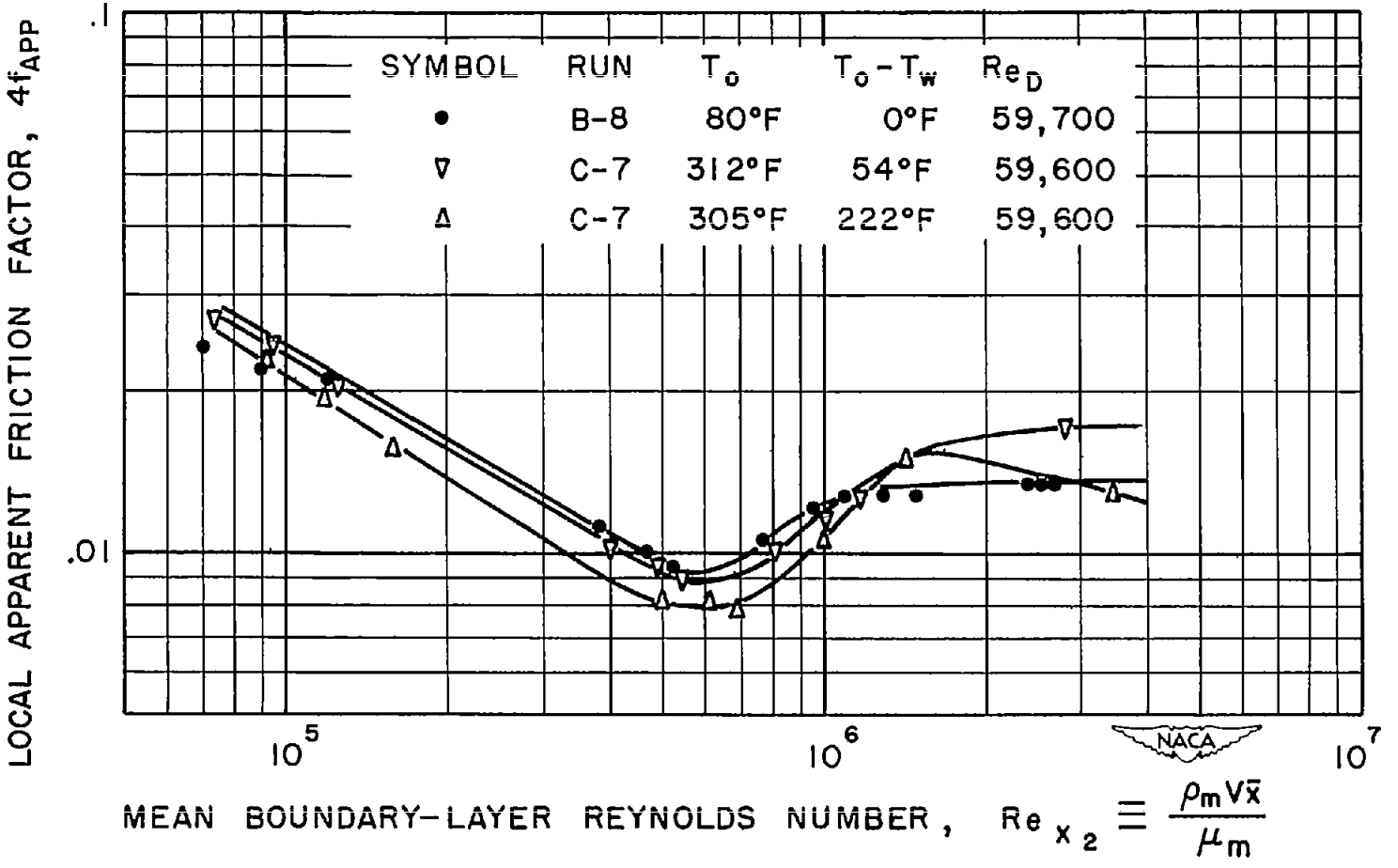

(i) Flow rate above pulsation with $Re_D \approx 60{,}000$. Same as figure 5(d) except that mean boundary-layer Reynolds number is used in place of free-stream Reynolds number.

Figure 5.- Continued.

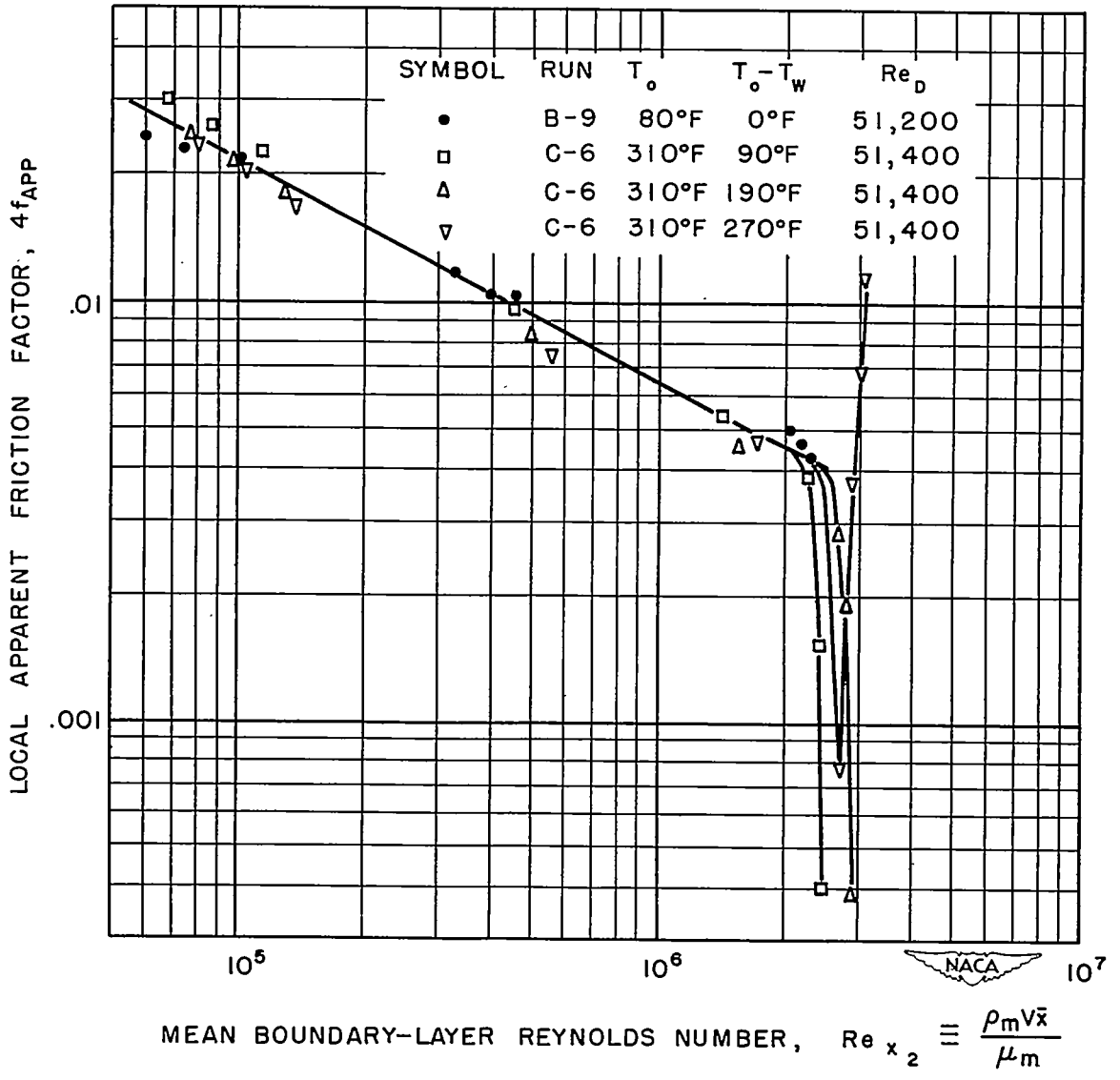

(j) Flow rate below pulsation with $Re_D \approx 51{,}000$. Same as figure 5(e) except that mean boundary-layer Reynolds number is used in place of free-stream Reynolds number.

Figure 5.- Concluded.

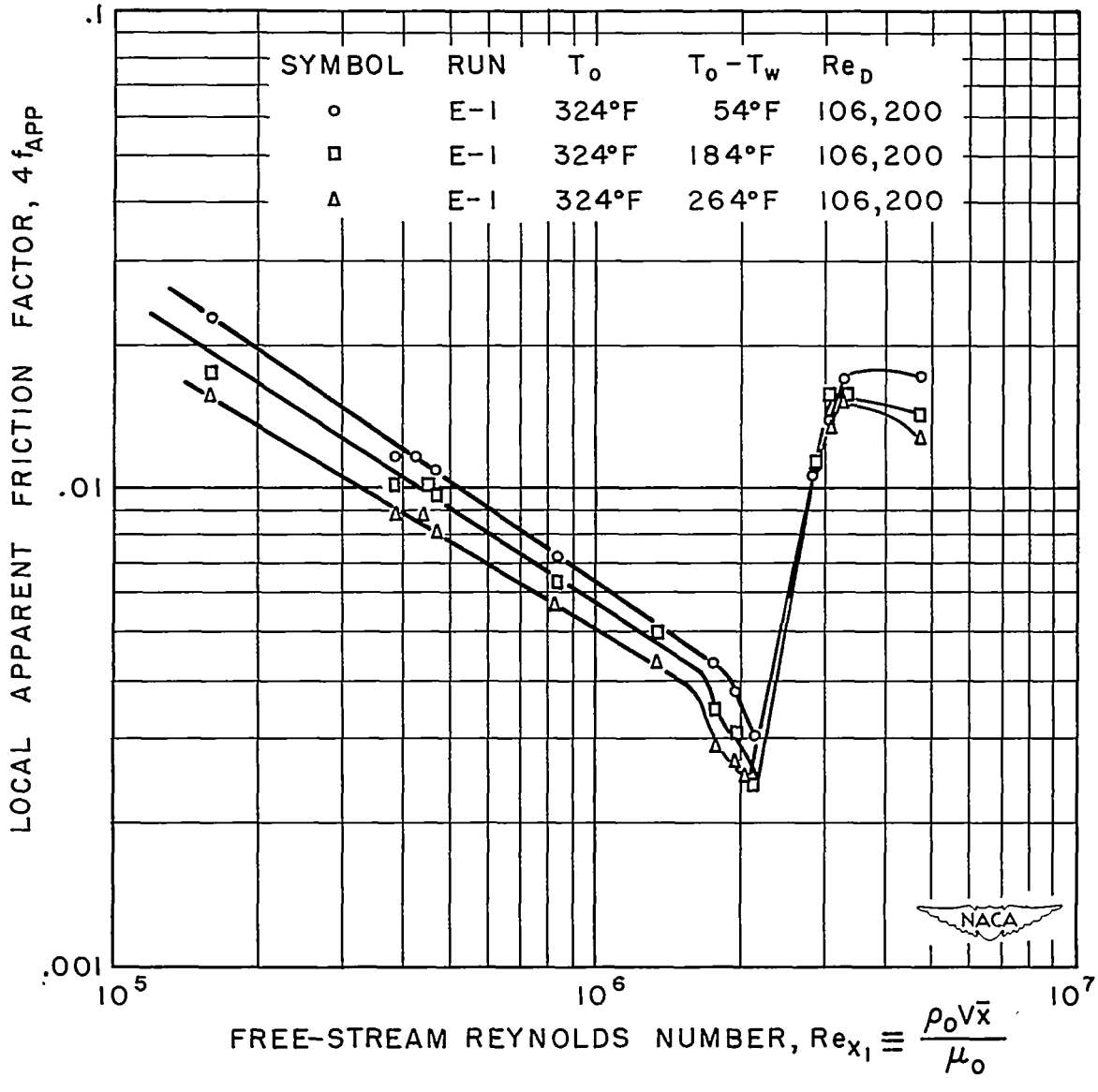

(a) Flow rate above pulsation with $Re_D \approx 106{,}000$.

Figure 6.- Effect of cooling on transition. Second group of runs with constant boundary-layer suction flow.

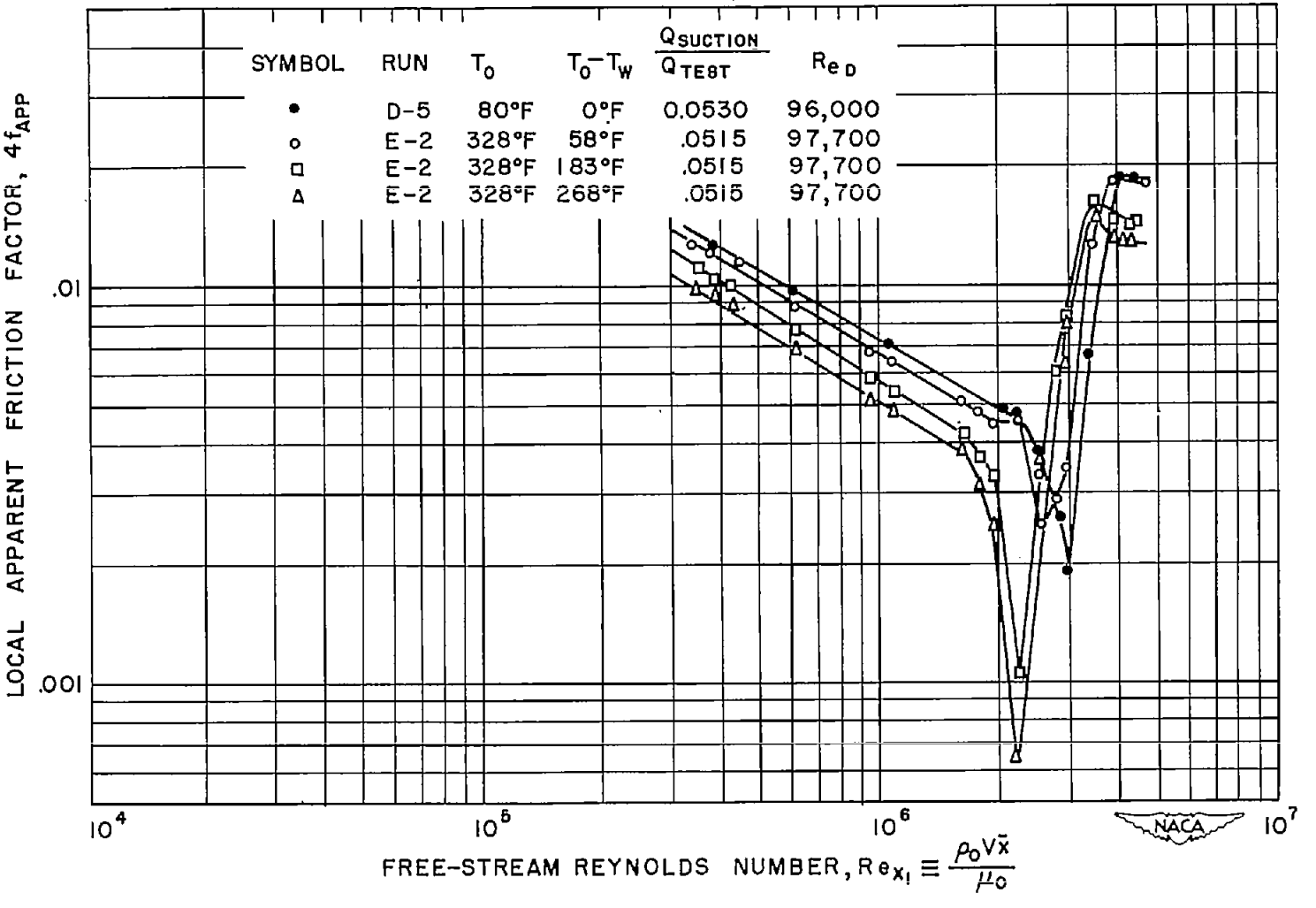

(b) Flow rate above pulsation with $Re_D \approx 97{,}000$.

Figure 6.- Continued.

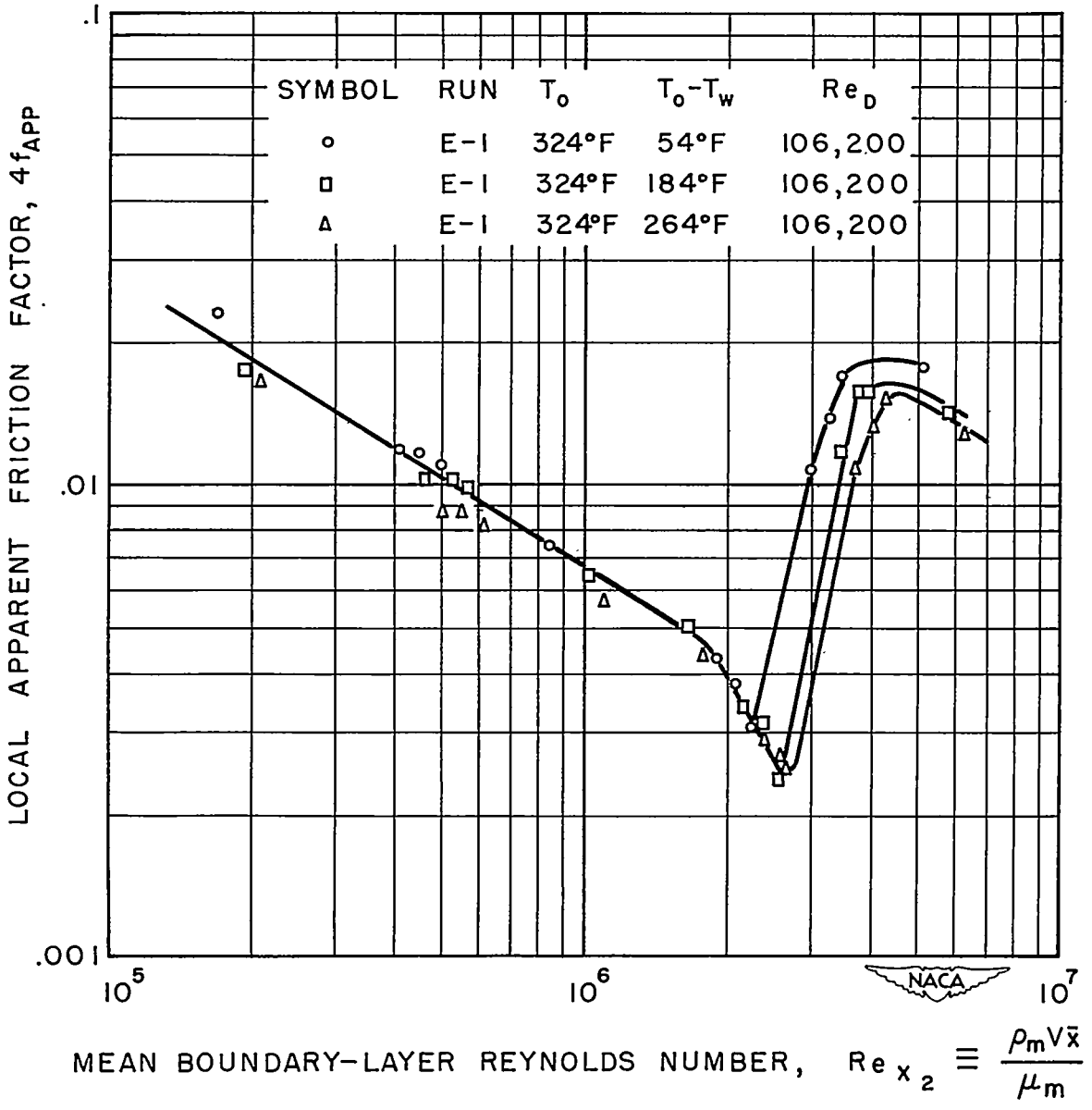

(c) Flow rate above pulsation with $Re_D \approx 106{,}000$. Same as figure 6(a) except that mean boundary-layer Reynolds number is used in place of free-stream Reynolds number.

Figure 6.- Continued.

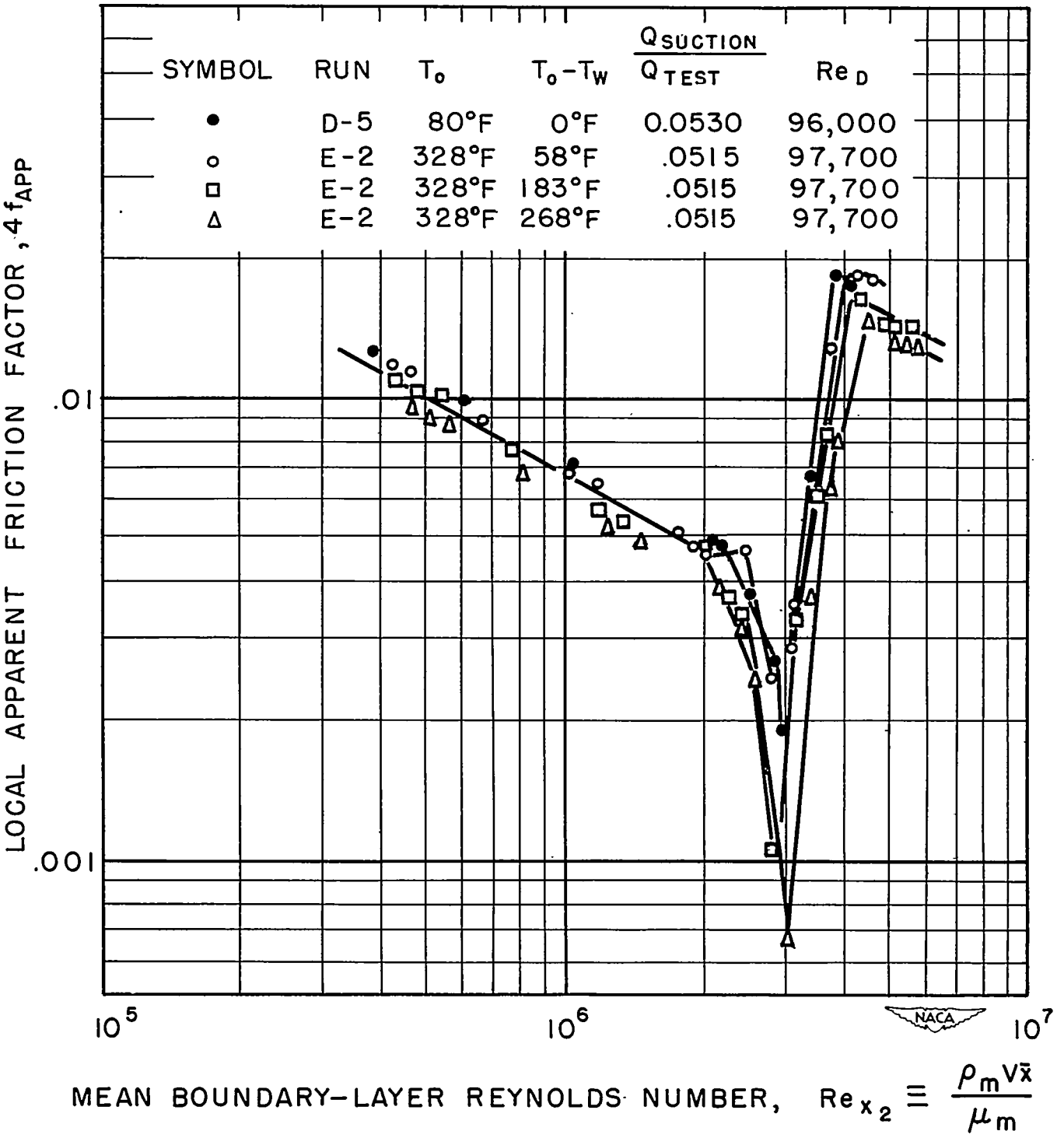

(d) Flow rate above pulsation with $Re_D \approx 97{,}000$. Same as figure 6(b) except that mean boundary-layer Reynolds number is used in place of free-stream Reynolds number.

Figure 6.- Concluded.

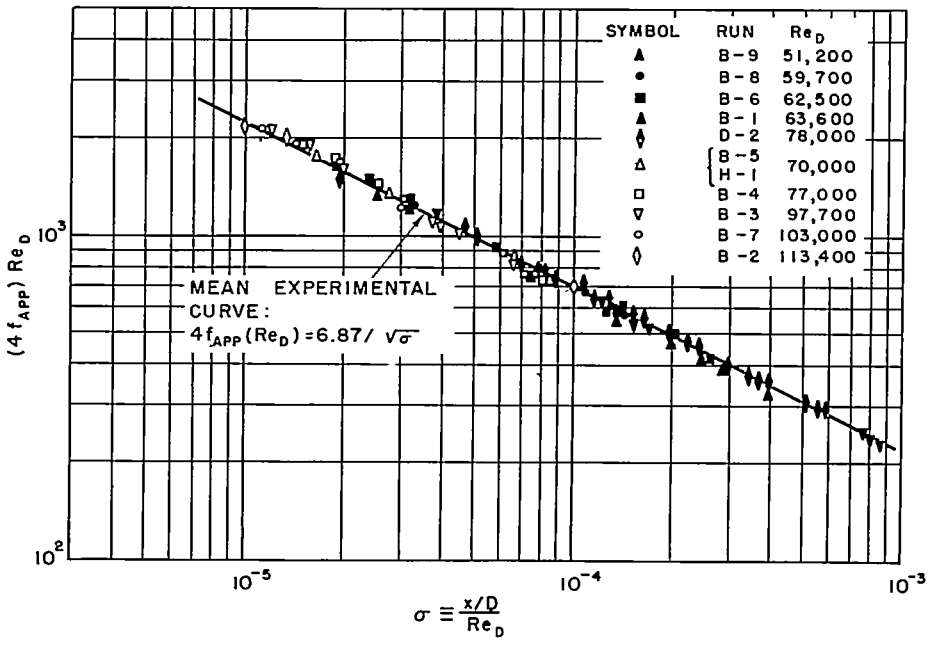

(a) Plot of all data showing mean experimental curve.

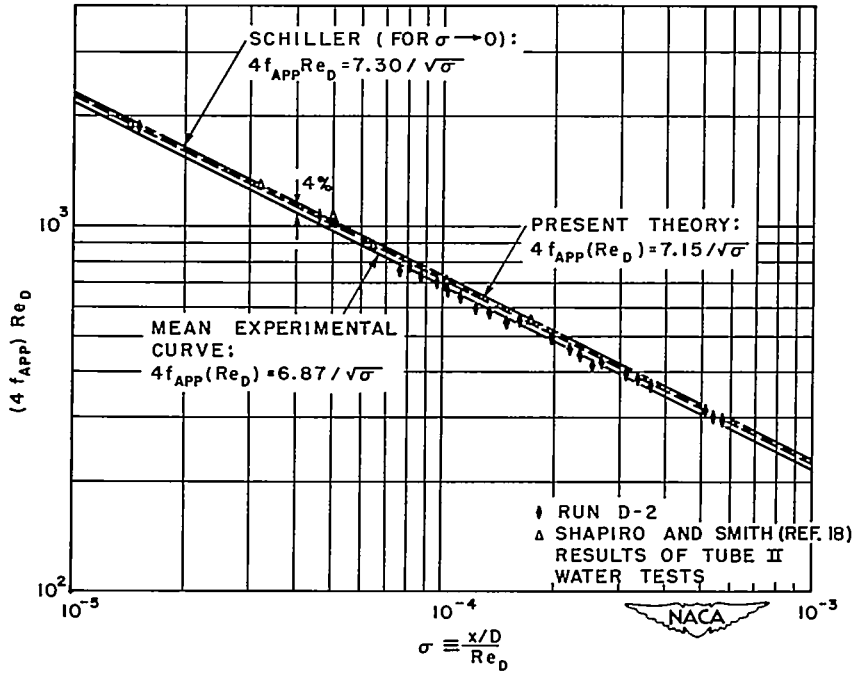

(b) Comparison of mean experimental curve with best run (run D-2), with data of Shapiro and Smith (ref. 18), with the theory of Schiller (ref. 25), and with present theory.

Figure 7.- Generalized correlation of local apparent friction factor in laminar entrance zone for all adiabatic data.

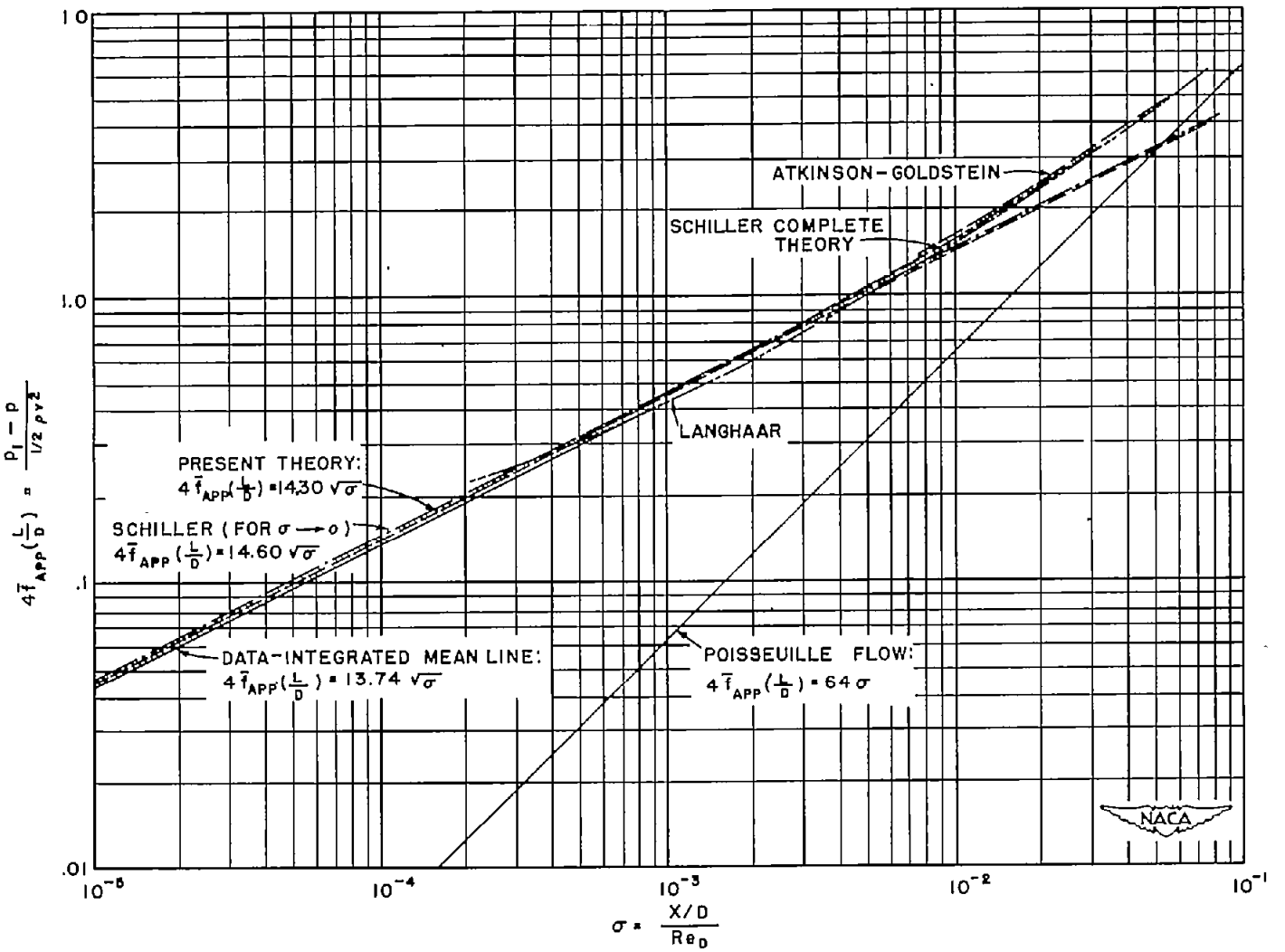

Figure 8.- Comparison of theories with integrated mean experimental curve of local apparent friction factor for laminar entrance zone.

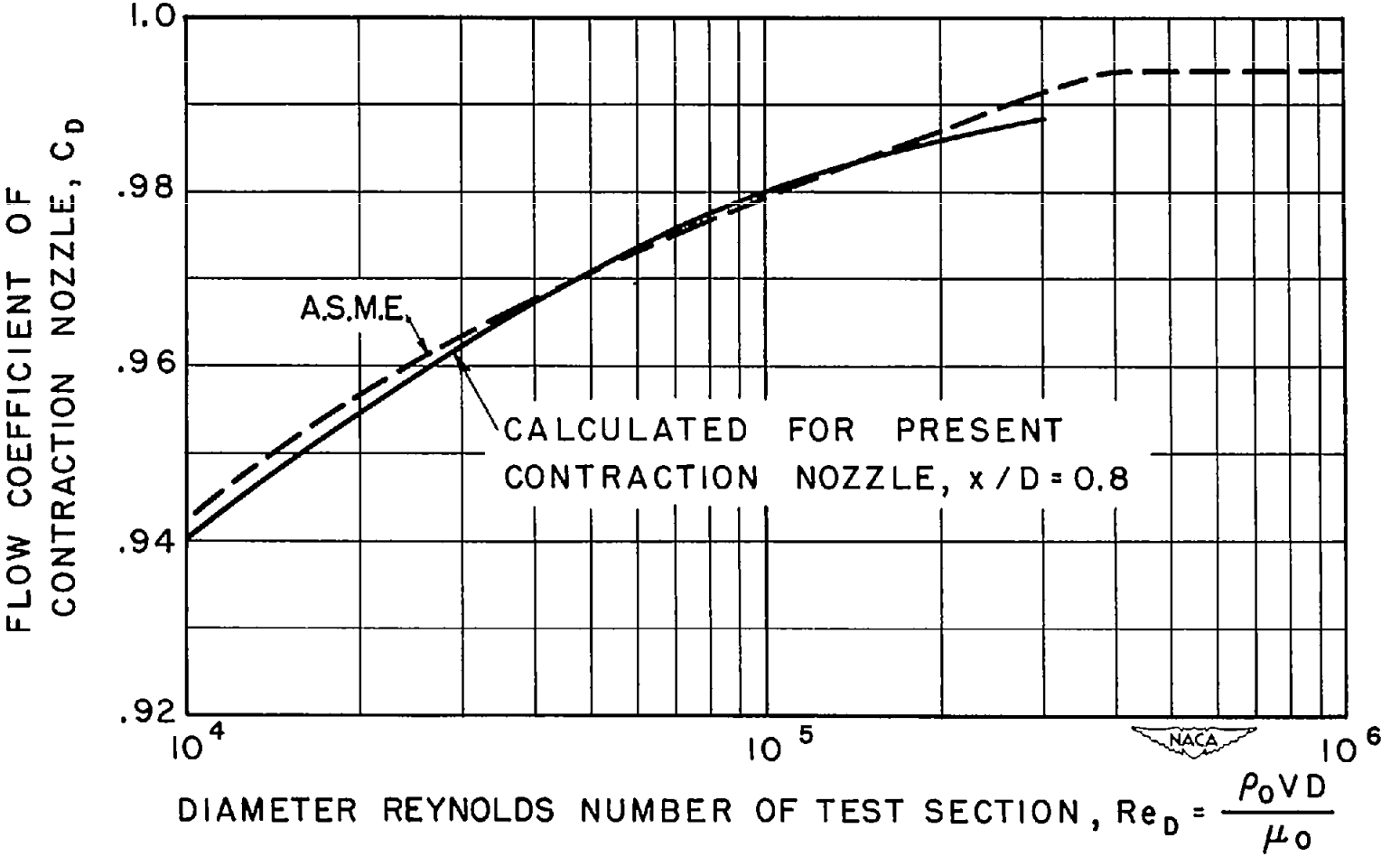

Figure 9.- Calculated flow coefficient of contraction nozzle as a function of diameter Reynolds number of test section and comparison with empirical curve recommended by the A.S.M.E.

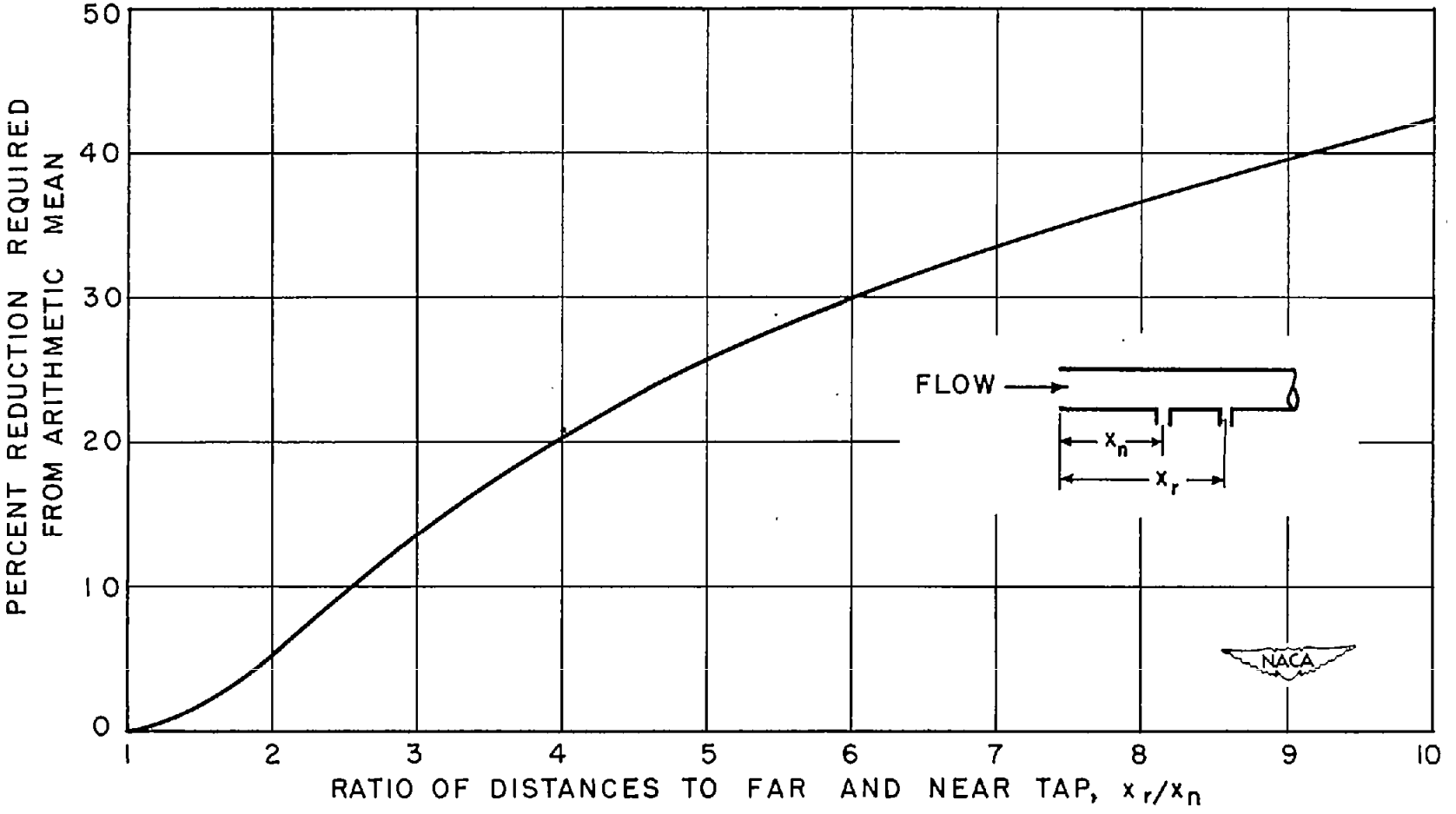

Figure 10.- Correction required to arithmetic mean of tap distances for proper $\bar{x}$ in laminar flow near entrance of tube.